CHAPTER – 3

SYNTHESIS AND CHARACTERIZATION OF iPP/ABS BLENDS

CONTENTS

3.1 Toughening mechanism in thermoplastics

It is well established that rubber particles with low moduli act as stress concentrators in both thermoplastics and thermoset resins, enhancing shear yielding and/or crazing, depending on the nature of the matrix.

Shear yielding in a polymer matrix involves macroscopic drawing of material without change in volume and the process takes place at an angle of about 45^0 to the tensile axis. For shear yielding to occur the presence of a shear stress is required as given by the Von Mises criterion[1]. The stress concentrations produced by elastomeric particles give the initiation sites for the various deformations, such as crazing, shear yielding in the form of shear band and elastic deformation. Crazing is the first step towards fracture in the polymers. Crazing, on the other hand, is a more localized form of yielding and occurs in planes normal to the tensile stress. These are voids at the crack tip interconnected by highly drawn fibrils which also form the craze walls and contain approximately 50% voids ranging in size from 20 A^0 to 200 A^0 [2]. Crazes grow by microscopic internal drawing of materials from the craze walls so as to increase the fibril length. It is initiated by a region of high stress concentration due to flaws or polymeric inclusions such as rubber particles.

The theory of multiple crazing in rubber toughened thermoplastic was proposed by Bucknall and Smith[3]. According to which, crazes are initiated at points of maximum principal strain, which is usually near the equator of the rubber particles and they propagate outwards along the plane of maximum principal strain. The process is terminated when the stress concentration falls below the critical level of propagation, or when a large particle or other obstacle is encountered. Thus the rubber particles are able to control craze growth by initiating and terminating crazes. Later on Bucknall et.al.[4] proposed that shear yielding and massive crazing are the two energy absorbing mechanisms in rubber modified plastics. Accordingly

the areas of stress concentration produced by rubber particles are initiation sites for shear band formation as well as for crazes and shear yielding is not simply an additional deformation mechanism but is an integral part of the toughening mechanism. As the number of shear bands increase, the length of newly formed crazes decreases. Consequently a large number of short crazes are generated. In polymers which form crazes and shear bands readily, the interaction between the two increases the overall toughness of the material.

The process of voiding as a toughening mechanism has been suggested by some workers[5-8]. There is very little published work on the fracture properties of thermoplastic containing voids. The ability of voids to lower the hydrostatic tension at the crack tip was suggested by Hobbs[6] and he found that the fracture toughness of glass-filled polycarbonate foam increases with increasing void content. Suggested mechanism was that the presence of voids reduces the hydrostatic constraints and allows some shear yielding to occur in the cell wall. The occurrence of a matrix voiding as a mechanism of toughening was proposed by Maxwell and Yee[7]. According to them in some thermoplastics which failed predominantly by shear yielding the local build-up of hydrostatic stress at the crack tip is relieved by process of voiding. The initiation of voids and their subsequent growth enhances the matrix flow. They have also pointed out that toughening by voiding occurs most readily in polymers whose matrices are ductile but notch sensitive (e.g. PC). Similar toughening mechanism was also reported for the rubber modified nylon-6 blend system[8].

3.1.1 Factors affecting toughening mechanism

Toughening mechanism of the blends is expressed in terms of fracture behaviour. Hence factors affecting fracture behaviour are discussed below.

(1) Adhesion

The adhesion between the dispersed phase and matrix plays an important role in determining the final impact strength of resultant blends. If the adhesion between the two phases is inadequate a void is formed at the interface and a crack formation is initiated. If one such crack is developed it is transferred from one particle to other with little hindrance from poorly anchored particles in its path. Thus, under impact condition the material will show very poor impact behaviour. However, according to Wu[9] strong adhesion does not always ensure toughening. The optimum adhesion required should be such that, the elastomeric particles are not detached from matrix during fracture.

(2) Particle size

The size of the dispersed particles has noticeable effect on the toughness of the blends. For each type of polymeric blends there appears to be an optimum particle size for toughening. Impact strength falls drastically if average particle diameter is reduced below the optimum value. The smaller particles are unable to initiate the craze formation and also to control craze growth effectively. Again the particle size must exceed the craze thickness to prevent the dispersed phase from becoming encapsulated in the growing craze. Impact strength also falls drastically if the particle size is increased above the optimum diameter due to increased distance between neighboring particles resulting into increase in craze size. Again the higher particle size can limit the shear bending and cavitation process. Therefore, the lower particle size of dispersed phase is favoured. Here smaller particles are small enough to control crazing directly and large enough to control it indirectly by initiating shear yielding.

(3) Matrix ligament thickness

The matrix ligament thickness is the average surface to surface interparticle distance. According to Wu[10] for pseudo ductile matrix, the matrix ligament thickness should be always lower than critical matrix ligament thickness (T_c), for achieving the improved toughening with the soft dispersed phase. T_c is the characteristic of the matrix alone at a given temperature and rate of deformation, but independent of domain size and volume fraction of the dispersed phase. According to Wu[10] if matrix ligament thickness is thinner than T_c a plane strain to plain stress transition occurs resulting into the ligament shear yield and hence blend toughening. On the other hand, if the ligament is thicker than T_c, such transition does not occur and matrix ligament shows brittleness.

(4) The dispersed phase properties

The stress for elastomer required to cavitate in a triaxial stress state decreases with decreasing its tensile modulus. Thus, the elastomers having lower tensile moduli are more effective in improving impact behavior.

3.2 Various theories predicting the tensile modulus of the heterogeneous blends

Theoretical models for the tensile modulus of heterogeneous blends.

Many theories have been proposed for predicting the tensile modulus of heterogeneous blends[11]. There are three principle groups of models that can predict the modulus - composition dependence of blends.

(i) Mechanical coupling model,
(ii) Self consistent model,
(iii) Bounds on modulus model.

In principle, mathematical models describing the mechanical response in terms of properties of blends constituents allow identification of responses that can be accounted for on purely mechanical ground.

(i) Mechanical coupling model

The mechanical coupling model is an empirical expression, containing an adjustable parameter. It furnishes a convenient frame work for empirical curves fitting and systematic phenomenological description of blend behavior. The major drawback for use of this model is attributing a physical meaning to the adjustable parameter as it is not morphologically or mechanically realistic model.

(ii) Self consisting model

The Self consisting model is based on the following assumptions.

- Perfect adhesion exists between the matrix and the inclusion (dispersed phase).
- Negligible interaction takes place between the dispersed phase particles and
- Dispersed phase particles embedded in matrix are spherical in shape and are isotropic morphologically and mechanically.

Based on these, Kerner's[12] model was originally developed for the shear modulus of a composite consisting of particulates and polymer matrix. However, this model is useful for the prediction of the tensile modulus of a certain class of heterogeneous blend systems. When the matrix and inclusion have the same Poisson's ratio, the Kerner's model for a system having perfect adhesion at the boundary may be written as :

$$E_b = E_m \frac{\{\phi_d E_d/[(7-5\nu_m) E_m + (8-10\nu_m) E_d] + \phi_m/15 (1-\nu_m)\}}{\{\phi_d E_m/[(7-5\nu_m) E_m + (8-10\nu_m) E_d] + \phi_m/15 (1-\nu_m)\}} \quad (1)$$

Here, E is the tensile modulus, ϕ is the volume fraction and ν is Poisson's ratio. The subscripts b, m and d refer to the blend, the matrix and the dispersed phase respectively. The Poisson's ratio for ABS and iPP are 0.39 and 0.35 respectively. These values are close enough to use the Kerner's equation in the above form.

For the polymeric system in which dispersed phase particles are loosely bound, $E_d = 0$ and eq.(1) is reduced to

$$\frac{1}{E_b} = \frac{1}{E_m}\left[1 + \frac{15(1-\nu_m)\phi_d}{(7-5\nu_m)\phi_m}\right] \quad (2)$$

It should be noted that in the Kerner's derivation only particle – matrix adhesion, but no particle–particle interaction was assumed. Therefore, the Kerner's model may not be applicable to the polymer blend system in which strong interaction between particle-particle may exist.

For such type of polymer system, Nielsen[13] suggested a modification of the Kerner's model. According to Nielsen[13]

(i) For a rigid polymer dispersed in a rubber matrix

$$\frac{E_b}{E_m} = \frac{1 + AB\phi_d}{1 - B\psi\phi_d} \quad (3)$$

in which,

$$B = \left[\frac{E_d}{E_m} - 1\right] / \left[\frac{E_d}{E_m} + A\right]$$

$$\psi = 1 + \left[\frac{(1 - \phi_{max})}{\phi^2_{max}} \right] \phi_d$$

(ii) For rubber inclusion in a rigid matrix

$$\frac{E_m}{E_b} = \frac{1 + A B_i \phi_d}{1 - B_i \psi \phi_d} \qquad (4)$$

where $$B_i = \left[\frac{E_m}{E_d} - 1 \right] / \left[\frac{E_m}{E_d} + A \right]$$

ϕ_{max} is the maximum packing volume and can be considered as a scale of interaction between two phases. A small value of ϕ_{max} represents a large extent of the interface, which is immobilized by dispersed phase. The constant A in eq.(3) and eq.(4) takes into account the geometry of the particulate phase. For spherical dispersed phase particles and for the two phases having the same Poisson's ratio, the constant A is $(7 - 5\nu_m) / (8 - 10\nu_m)$ for eq.(3) and $(8 - 10\nu_m) / (7 - 5\nu_m)$ for eq.(4).

The approach of self consistent model for the prediction of the tensile modulus values of various blends, mainly relies on the simplified assumptions about the morphology and physical behavior of the blends. It predicts approximate but single valued modulus for each blend.

(iii) Bounds on modulus model

According to Paul[14], the bounds on modulus model represents an alternate approach based on the variational principle to bound the strain energy and thus to place upper and lower limits on the moduli of the blends.

According to Paul upper limit is given by

$$E_b = (1 - \phi_d) E_m + \phi_d E_d \qquad (5)$$

and lower limit by,

$$E_b = 1 \Big/ \left[\frac{(1 - \phi_d)}{E_m} + \frac{\phi_d}{E_d} \right]$$

3.3 Experimental

The isotactic polypropylene (iPP) of M0030 Koyelene grade with density 0.93 g/cm^3 and melt flow index(MFI) 10 g/10 min at 2.16 kg load was supplied by Indian Petrochemical Corporation Ltd., Vadodara, India. Before blending iPP was dried in hot air oven at 70 ^{0}C for 12 h.

Acrylonitrile–butadiene–styrene(ABS) of 100 Natural grade with 1.05 g/cm^3 density and melt flow index 10 g/10 min. at 10 kg load was supplied by Bayer ABS Ltd., Vadodara, India and was dried in hot air oven at 70 ^{0}C for 12 h.

Compatibilizers iPP-g-methacrylic acid and HPP-g-STY-MMA were also dried in a hot air oven before extrusion.

3.3.1 Preparation of blends

All the blends of iPP and ABS were prepared by melt mixing technique. The Brabender plasticorder system coupled with single screw extruder (L/D = 20) was used for the preparation of the blends. All the blends were prepared by two step mixing technique. In first step,

polypropylene and compatibilizer (iPP-g-methacrylic acid) with 1:1 wt/wt ratio were premixed in the extruder keeping the temperature of four zones at 190 – 200 – 210 – 220 ^{0}C and screw speed at 50 rpm. In the second step the resultant mixture was palletized and calculated amount was mixed with ABS and iPP in the extruder with screw speed 50 rpm and keeping the zone temperatures at 200 – 220 – 230 – 225 ^{0}C for iPP–rich compositions and 220 – 230 – 250 – 240 ^{0}C for ABS–rich compositions. Various blend compositions studied are given in Table 3.1 and Table 3.2 Here, the extrudate was obtained in the form of a thread, which was quenched in water, dried and granulated. For all the blends, during mixing, the initial extrudate was discarded in order to ensure steady operation and to flush out impurities from the extruder to ensure the resulting blend free from any impurities adhered to the extruder.

3.3.2 Specimen preparation

The blend pallets were injection moulded using "ARBURG ALLROUNDER–220–90–350" injection moulding machine to obtain the test specimen for the measurements of mechanical properties and were prepared as per the ASTM standard.

3.3.3 Characterization of blends

3.3.3.a Scanning electron microscopy

The morphology of room temperature fractured surface of izod test bars, etched either with methyl ethyl ketone (MEK) for ABS extraction or hot xylene for iPP extraction was examined using scanning electron microscope(SEM) (Leica Cambridge, UK., Stereoscan) at 10 kV. The samples were coated with gold (50 μm thick) using automatic sputter, coater (Polaron equipment Ltd., USA) to avoid surface charging.

The size of the ABS domains measured from the SE-micrographs is expressed in different ways, such as,

Table 3.1 : Compositions of iPP/ABS/HPP-g-STY-MMA blend systems

iPP/ABS (%)	iPP/ABS/ HPP-g-STY-MMA* (%)	iPP/ABS/ HPP-g-STY-MMA* (%)	iPP/ABS/ HPP-g-STY-MMA* (%)
100/0	-	-	-
90/10	90/10/2.5	90/10/5.0	90/10/7.5
85/15	85/15/2.5	85/15/5.0	85/15/7.5
75/25	75/25/2.5	75/25/5.0	75/25/7.5
25/75	25/75/2.5	25/75/5.0	25/75/7.5
15/85	15/85/2.5	15/85/5.0	15/85/7.5
10/90	10/90/2.5	10/90/5.0	10/90/7.5
0/100	-	-	-

* HPP-g-STY-MMA was added as a compatibilizer in parts per hundred of resin(phr)

Table 3.2 : Compositions of iPP/ABS/iPP-g-MAA blend systems

iPP/ABS (%)	iPP/ABS/ iPP-g-MAA* (%)	iPP/ABS/ iPP-g-MAA* (%)	iPP/ABS/ iPP-g-MAA* (%)
100/0	-	-	-
90/10	90/10/2.5	90/10/5.0	90/10/7.5
85/15	85/15/2.5	85/15/5.0	85/15/7.5
75/25	75/25/2.5	75/25/5.0	75/25/7.5
25/75	25/75/2.5	25/75/5.0	25/75/7.5
15/85	15/85/2.5	15/85/5.0	15/85/7.5
10/90	10/90/2.5	10/90/5.0	10/90/7.5
0/100	-	-	-

* iPP-g-MAA was added as a compatibilizer in parts per hundred of resin(phr)

$$\overline{D}_n = \Sigma N_i D_i / \Sigma N_i$$

$$\overline{D}_w = \Sigma N_i D_i^2 / \Sigma N_i D_i \quad \text{and}$$

$$PDI = \overline{D}_w / \overline{D}_n$$

Where, N_i is the number of domains, $\overline{D}_n$ is the number-average diameter and $\overline{D}_w$ is weight average diameter. The polydispersity index, which is a measure of domain size distribution is also calculated from the above equations

3.3.3.b Tensile properties measurements

Tensile properties of the dumbbell shaped test specimens having the dimensions of the narrow portion 57 x 13 x 3.2 mm were measured according to ASTM–D–368 procedure. At least 5–6 specimens were tested for each sample. The specimens, which do not break between pre-determined gauge marks, or that break at some obvious fortuitous flaw were discarded. All testing was carried out at 50 mm/min cross head speed. Stress–strain curves, young modulus flexural strength, tensile strength, % elongation were obtained on the Instorn tester attached to computer.

3.3.3.c Impact strength measurement

The test samples having dimensions 64 x 128 x 3.2 mm with 0.25 mm notch in radius were used for the izod impact strength measurement. The measurements were carried out according to ASTM–D–256 method using at least 5–6 individual test specimens to obtain the average impact strength.

3.3.3.c Flexural strength measurement

Flexural measurement was carried out according to the method described in ASTM–D–790. Three point loading system with a central loading

on a single supported beam was used for the measurements. The test samples were of 125 x 12.2 x 6.2 mm dimensions. During testing the rate of cross head motion was kept at 2.8 mm/min. At least five individual determinations of flexural strength were made on each sample.

3.3.3.d Melt flow index (MFI) measurement

MFI is quoted as weight expelled in g per 10 min. MFI has inverse relationship with molecular weight. It gives an idea about ease of processing.

MFI of iPP and ABS and their blends was determined by using a Melt Flow Matic (MFM), made by Ceast, Italy. It has a capillary die of length 8.0 mm, diameter 2.095 mm and driving weight of 2.16 kg.

MFI was measured at 220 ^{0}C temperature. The melt through the die was cut at a measuring length of 25.4 mm and five such samples were taken and weighted twice and the average value of MFI was reported.

3.3.3.e. Rheology

Shear melt viscosity was measured using Rheologic-1000 instrument made by Ceast, Italy at 220 ^{0}C temperature using L/D=20 and shear rates, R= 50, 100, 200, 500, 1000, 2000 and 5000 s^{-1}. The test sample was placed inside the barrel of the extrusion assembly and forced down into the capillary with the piston attached to the moving crosshead after preheating upto 4 min. Sample was preheated for 2 h at 70 ^{0}C temperature in air circulating oven before performing the test.

3.4 Results and discussion

Immiscibility between polymer components is responsible for the poor–phase structure and mechanical performance, which is the main

hurdle for the development of high performance blends. Therefore, enhancement in the compatibility of immiscible polymer pairs is a key to obtain a polymer blend with desirable properties. It has been reported by various researchers[14-16] that iPP and ABS form immiscible mixture with each other. Attempts have been made to some extent to improve the miscilibility by using various compatibilizers. The compatibilization tried in our laboratory is discussed here.

3.4.1 HPP-g-styrene-methyl methacrylate (HPP-g-STY-MMA) as a compatibilizer for iPP/ABS blends

The synthesis and characterization of HPP-g-STY-MMA is discussed in Chapter 2. In this section the potential of HPP-g-STY-MMA as compatibilizer for iPP/ABS blends is discussed.

iPP and ABS form incompatible mixture. Addition of HPP-g-STY-MMA copolymer to iPP/ABS blends decreases the interfacial tension and acts as an emulsifier does in oil in water system. The different compositions of blends prepared are given in Table 3.1. The blends were further characterized for their morphological and mechanical properties.

3.4.1.a Morphology

Fig. 3.1.a and b show the scanning electron micrographs of room temperature impact fractured 90/10 and 75/25 % iPP/ABS binary blends after extraction of ABS inclusions from the iPP matrix in methyl ethyl ketone. In the binary blends, though the dispersion and distribution of ABS particles were observed to be uniform the size of ABS inclusions increases with increasing concentration of ABS. The particle size was observed to increase from 2.80 to 5.0 μm for the 90/10 and 75/25 % iPP/ABS blends. For the determination of the particle size of dispersed phase approximately 100 particles were selected for each system. The weight

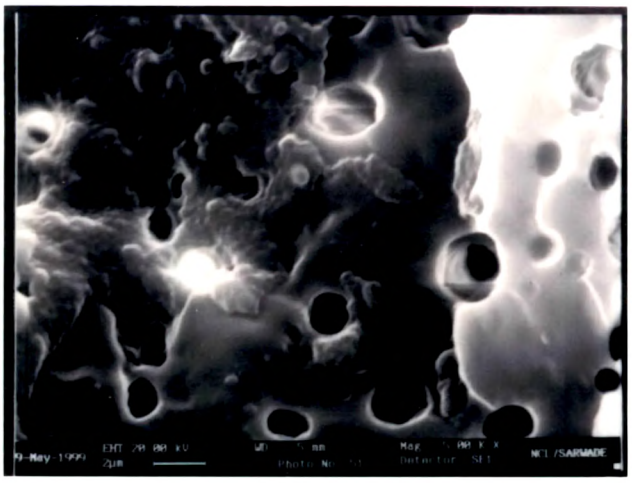

a

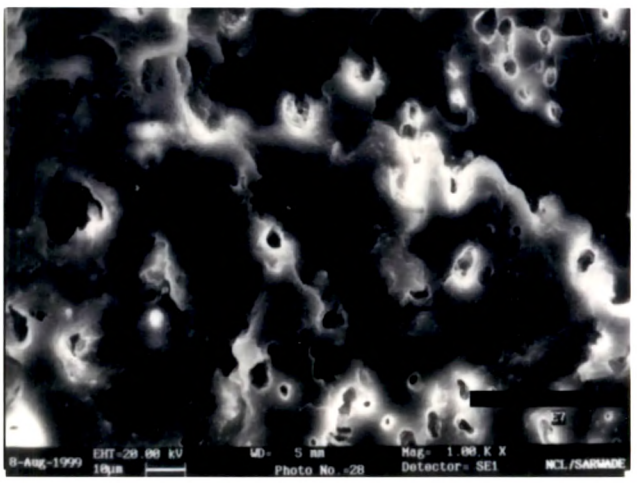

b

Figure 3.1 : SE micrographs of impact fractured surface of iPP/ABS blends

a : 90/10, iPP/ABS **b** : 75/25, iPP/ABS

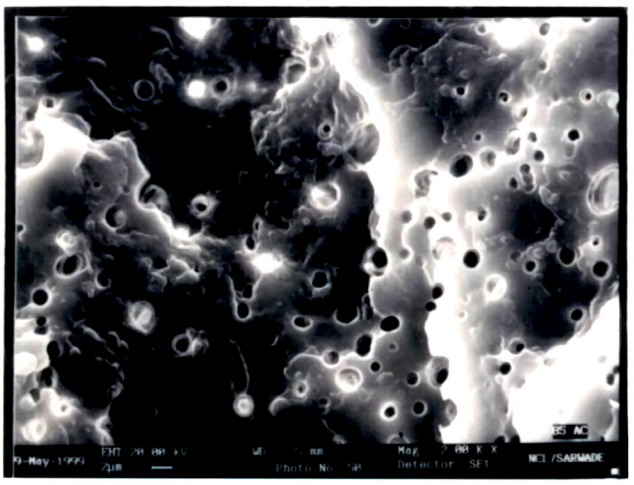

a

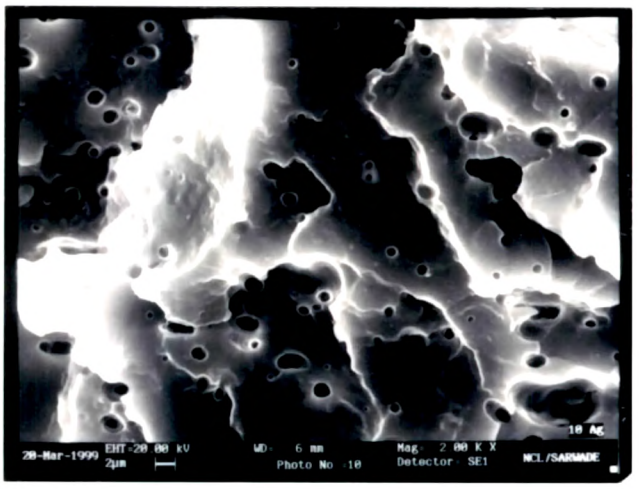

b

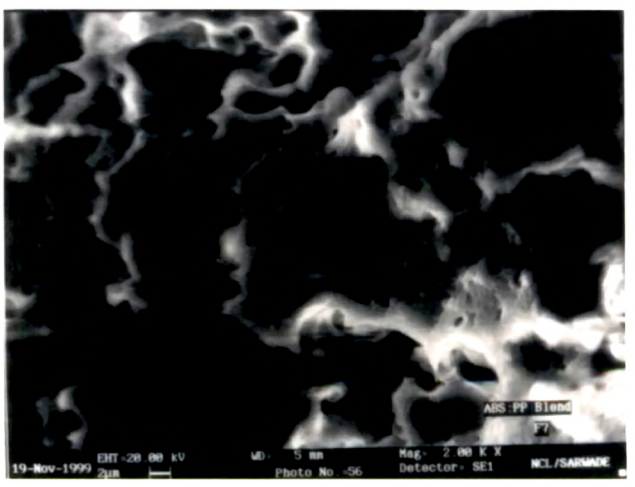

c

Figure 3.2 : SE micrographs of impact fractured surface of iPP/ABS/HPP-g-STY-MMA blends after extraction of ABS in MEK

a : 90/10/2.5 **b** : 90/10/5.0 **c** : 90/10/7.5 iPP/ABS/iPP-g-STY-MMA

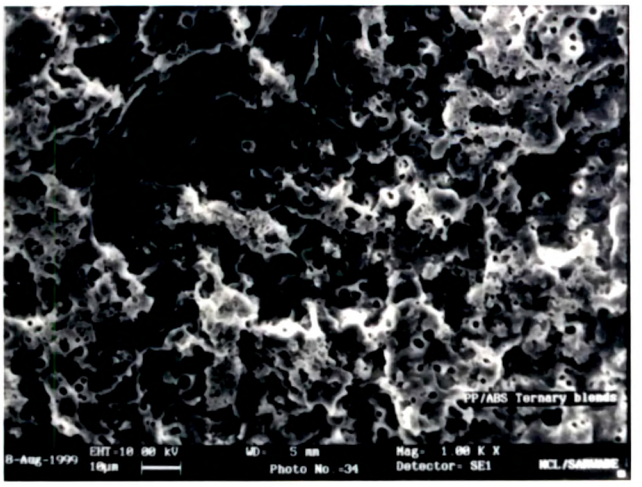

a

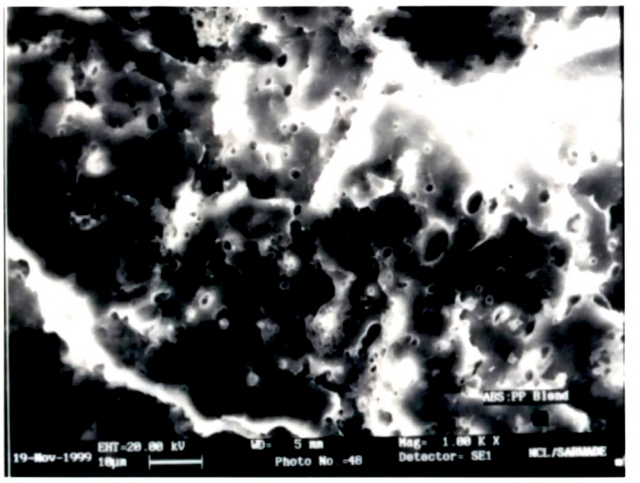

b

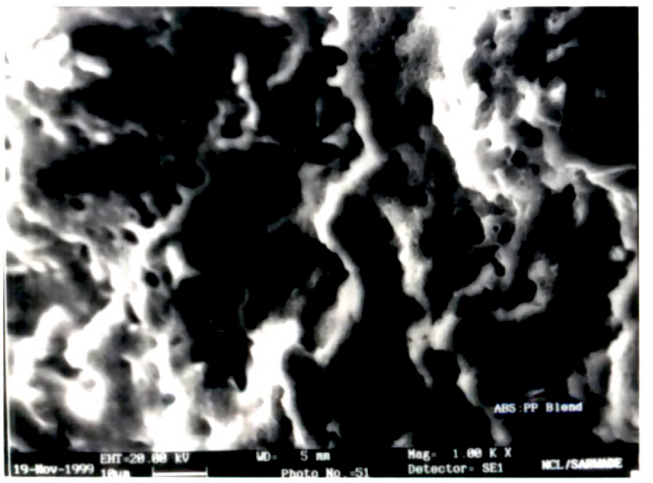

c

Figure 3.3 : SE micrographs of impact fractured surface of iPP/ABS/HPP-g-STY-MMA blends after extraction of ABS in MEK

a : 75/25/2.5 **b** : 75/25/5.0 **c** : 75/25/7.5 iPP/ABS/iPP-g-STY-MMA

Table 3.3 : Particle size and polydispersity index(PDI) for iPP/ABS/HPP-g-STY-MMA system

Blend composition iPP/ABS/ HPP-g-STY-MMA* (%)	$\overline{D}n(\mu m)$	$\overline{D}w(\mu m)$	PDI
90/10/0	2.80	2.28	0.81
90/10/2.5	1.49	1.56	1.05
90/10/5.0	1.82	2.16	1.18
90/10/7.5	2.23	2.51	1.13
75/25/0	5.0	5.78	1.15
75/25/2.5	2.7	3.01	1.11
75/25/5.0	3.05	3.23	1.05
75/25/7.5	3.10	4.49	1.45

* HPP-g-STY-MMA was added as a compatibilizer in parts per hundred of resin (phr).

average diameter($\overline{D}_w$), number average diameter ($\overline{D}_n$) and polydispersity index(PDI) are given in Table 3.3. Observed smooth surface between two phases in the binary blends indicates very little adhesion or no adhesion between iPP and ABS.

Fig. 3.2.a-c and Fig. 3.3.a-c show scanning electron micrographs of room temperature impact fractured surfaces of iPP/ABS/HPP-g-STY-MMA ternary blends of 90/10 and 75/25 % of iPP/ABS with 2.5, 5.0 and 7.5 phr HPP-g-STY-MMA copolymer as a compatibilizer. From the results given in Table 3.3, considerable decrease in particle size was observed in ternary blends, which can be attributed to the reduction in interfacial tension between matrix and inclusion. The observed rough surfaces of the cavities created during extrusion of ABS inclusions in ternary blends [Fig.3.2.a and Fig. 3.3.a] indicate increased adhesion between two phases. As the compatibilizer concentration increases from 2.5 to 5.0 phr the size of dispersed phase was observed to increase. This may be due to the formation of aggregates in the bulk phase above the critical miceller concentration (CMC). As a result poorly stabilized interface is formed which leads to larger dispersed particles [Fig. 3.2.c and Fig. 3.3.c]. Further increase in copolymer concentration upto 7.5 phr showed very small increase in the particle size. From the PDI it is observed that in ternary blends particles showed better polydispersity. To conclude, for 90/10 blend, 2.5 phr concentration of copolymer gives better morphology and mechanical properties. Similar trend was observed (Fig. 3.3.c) in 75/25 iPP/ABS blends compatibilised with 2.5, 5.0 and 7.5 phr of HPP-g-STY-MMA. However, at 7.5 phr iPP/ABS blend showed more co-continuous nature.

3.4.1.b Tensile properties

Fig. 3.4 shows the stress–strain behaviors of iPP, ABS, iPP/ABS binary and iPP/ABS/HPP-g-STY-MMA ternary blends. From the figure it is observed that virgin iPP shows behaviour like a soft and tough material, while ABS shows the behavior like hard and strong material. Incorporation of ABS

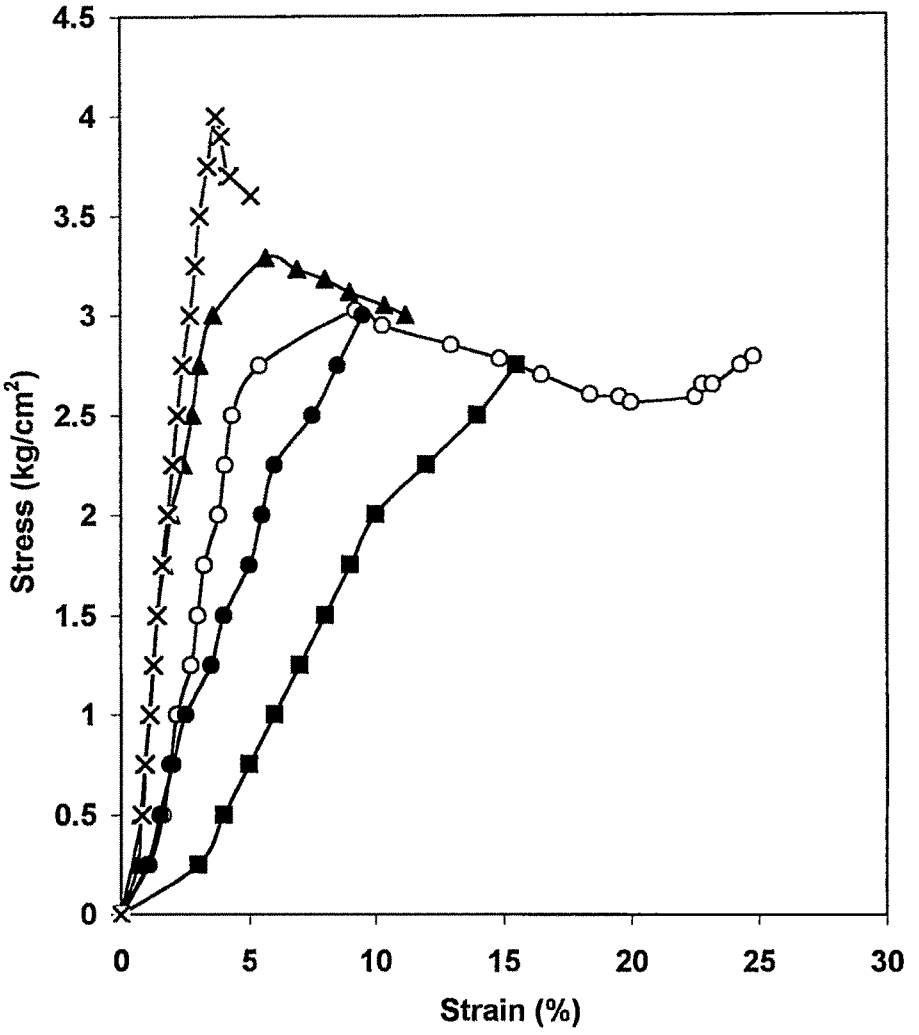

Figure 3.4 : Stress-strain dependence of iPP, ABS and iPP/ABS binary and ternary blend

(X) ABS

(o) iPP

(●) 90/10 iPP/ABS

(■) 75/25 iPP/ABS

(▲) 90/10/2.5 phr iPP/ABS/HPP-g-STY-MMA

into iPP matrix changes the property of the individual plastic such as cold drawing and ductility in iPP. Fig. 3.4 shows that a blend of 90/10 and 75/25 % iPP/ABS without compatibilizer behaves like a brittle and weak material. On incorporation of ABS into iPP the ductility of iPP decreases and brittle/weak character increases indicating poor adhesion between two surfaces. In ternary blends (90/10/2.5phr compatibilizer) the stress-strain curve linearly increases and it crosses the curve of virgin iPP indicating increased toughness of ternary blends. However, elongation at break decreases as compared to virgin iPP.

Tensile strength

Fig. 3.5 shows the tensile strength of iPP, ABS, iPP/ABS binary and iPP/ABS/HPP-g-STY-MMA ternary blends with 2.5, 5.0 and 7.5 phr of compatibilizer. From the data it can be observed that incorporation of 5 to 25 % of ABS in iPP matrix improves tensile strength of iPP whereas decreased tensile strength was observed on the incorporation of iPP into ABS. Hence, iPP–rich binary iPP/ABS and ternary iPP/ABS blends only show potential for commercial exploitation. On comparison of binary and ternary blends, it was observed that all ternary blends show superior properties than binary ones. However, on addition of 2.5 phr of HPP-g-STY-MMA graft copolymer as a compatibilizer maximum improvement in tensile strength of binary blends was achieved. Further increase in concentration of compatibilizer upto 7.5 phr did not show any improvement but lowered the tensile properties to some extent. This decrease in the tensile strength can be attributed to the saturation of polymer–polymer interface above 2.5 phr compatibilizer. At 2.5 phr compatibilizer concentration homogeneous dispersion and distribution of ABS in iPP matrix is obtained due to the accumulation of graft copolymer at the interface, which will result in an overall smaller size, i.e., finer dispersion of inclusion, (Fig. 3.2.a and Fig. 3.3.a and Table 3.3). At concentration above 2.5 phr due to the saturation at the interface, the excess of it goes to the bulk phase

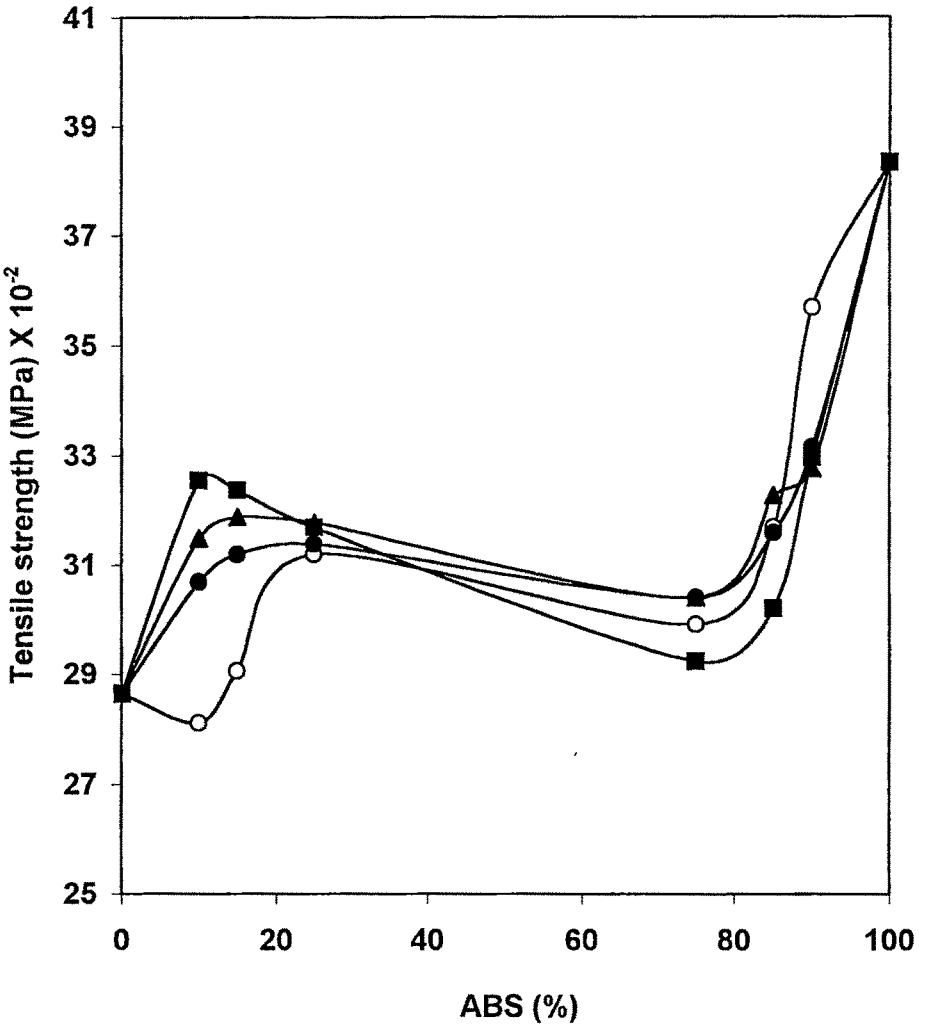

Figure 3.5 : Tensile strength of iPP/ABS binary and ternary blends

(o) iPP/ABS binary blends

(■) HPP-g-STY-MMA ternary blend (2.5 phr)

(▲) HPP-g-STY-MMA ternary blend (5.0 phr)

(●) HPP-g-STY-MMA ternary blend (7.5 phr)

leading to the formation of bigger particles of discrete ABS leading to poor dispersion as well as adhesion with ABS in iPP matrix which can be seen in Fig. 3.2.c and Fig. 3.3.c Similar results were observed by Masoud and Paul[15] and Han, et al.[16] for iPP/ABS and PA-6/PBT blend systems, respectively.

Fig. 3.6 shows tensile modulus of iPP, ABS, iPP/ABS binary and iPP/ABS/HPP-g-STY-MMA ternary blends. The increase in modulus values with increasing ABS content is due to higher tensile modulus of ABS itself. Whereas compatibilizer in ternary blends improves the homogeneity of system resulting into improved tensile modulus. This can also be seen in micrographs (Fig. 3.2.a and Fig. 3.3.a). The blend containing 2.5 phr HPP-g-STY-MMA graft copolymer as a compatibilizer with 10 to 15 % of ABS gave more homogeneity to the system and adhesion between inclusion and matrix, resulting into higher tensile modulus. The lower tensile modulus was observed for the blends containing 7.5 phr of HPP-g-STY-MMA graft copolymer as a compatibilizer, indicating that each system performs better at optimized concentration of compatibilizer.

The % elongation at break for iPP, ABS, iPP-rich iPP/ABS binary and corresponding ternary iPP/ABS/HPP-g-STY-MMA blends is given in Fig. 3.7. From the figure it is observed that all the binary/ternary blends with variable composition of ABS as well as concentration of compatibilizer have lower elongation values than that of polypropylene (iPP). Polypropylene is a crystalline material. Percentage elongation values express the capacity of the material to be plastically deformed by means of cold drawing which is observed in Fig. 3.4. The addition of ABS and/or functionalized–PP to iPP matrix can strongly modify the property like elongation. ABS particles develop hinderence to the cold drawing of iPP matrix and form a premature rapture of the specimen, due to poorer adhesion. On incorporation of 2.5phr compatilibilizer in 90/10 iPP/ABS an increase in elongation was observed, which indicates improved adhesion between two phases.

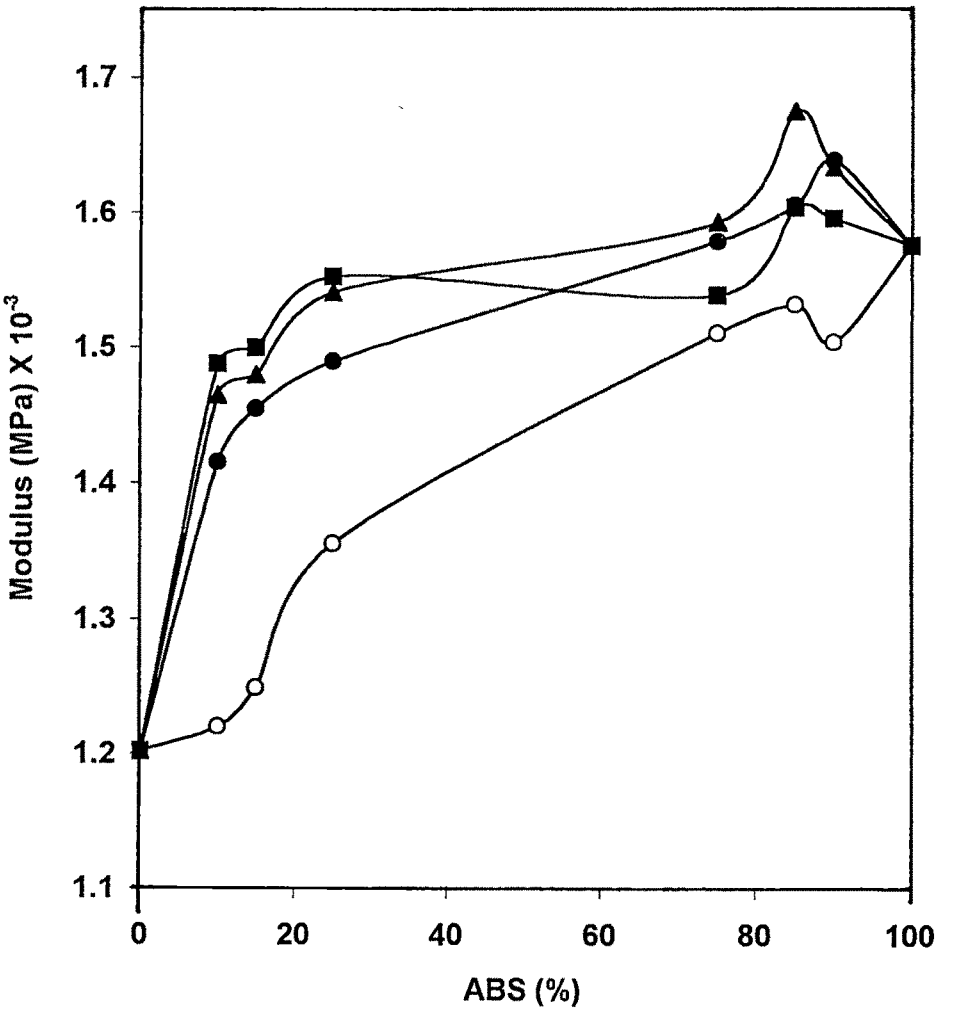

Figure 3.6 : Tensile modulus of iPP/ABS binary and ternary blends

(o) iPP/ABS binary blends

(■) HPP-g-STY-MMA ternary blend (2.5 phr)

(▲) HPP-g-STY-MMA ternary blend (5.0 phr)

(●) HPP-g-STY-MMA ternary blend (7.5 phr)

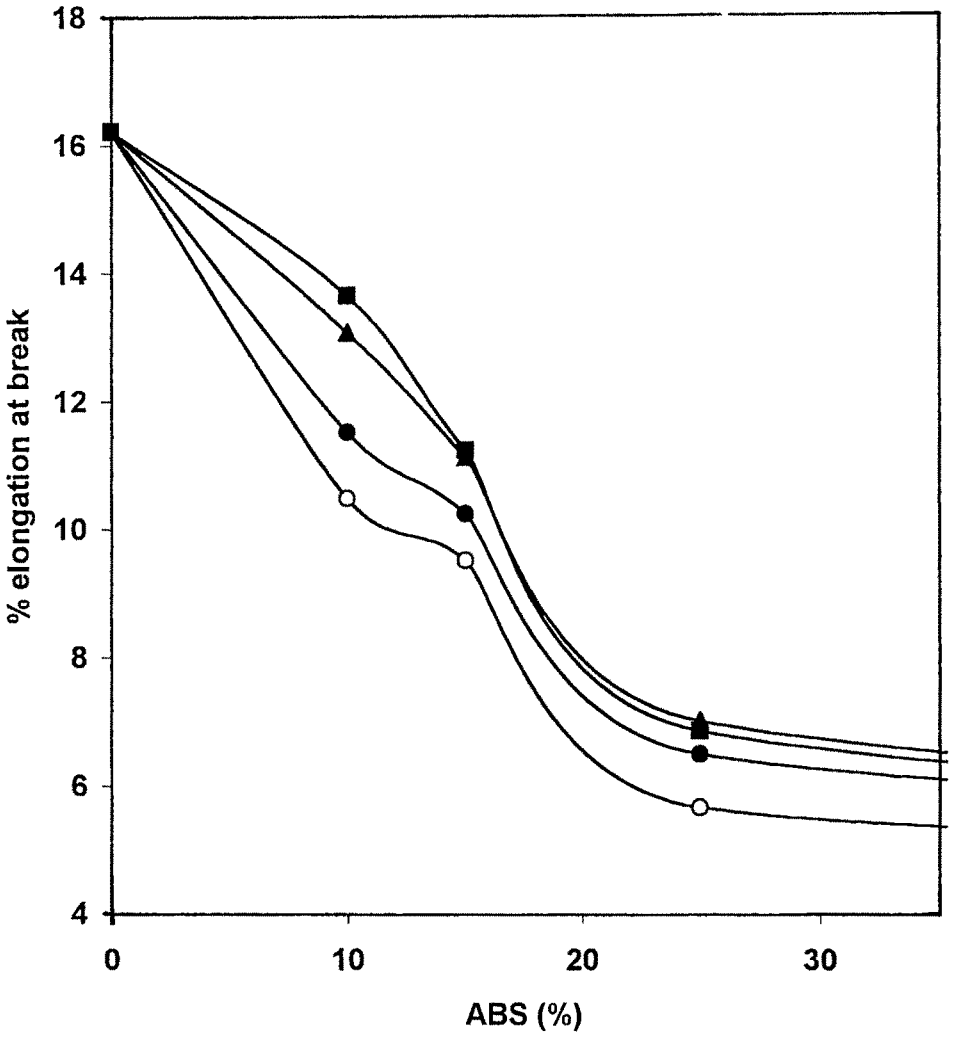

Figure 3.7 : % elongation at break of iPP/ABS binary and ternary blends

(o) iPP/ABS binary blends

(■) HPP-g-STY-MMA ternary blend (2.5 phr)

(▲) HPP-g-STY-MMA ternary blend (5.0 phr)

(●) HPP-g-STY-MMA ternary blend (7.5 phr)

3.4.1.c Impact strength

Fig. 3.8 illustrates the impact strength of iPP/ABS binary and iPP/ABS/HPP-g-STY-MMA ternary blends as a function of blend composition. From the figure it is clearly observed that compatibilized blends produce a higher impact strength than that of the corresponding binary blend. ABS has higher impact value, hence incorporation of ABS to iPP should increase the impact strength of iPP/ABS blends. However, no improvement was observed in iPP-rich binary blends but corresponding ternary blends showed an improvement in impact strength. This implies that the discrete ABS and/or iPP phase is not loosely bound with matrix and some adhesion forces exist between iPP and ABS in the presence of compatibilizer, which provides more stiffening effect, which can be attributed to the higher co-efficient of thermal expansion of iPP as compared to ABS (1.7×10^{-4} k^{-1} and 0.8×10^{-4} k^{-1} for iPP and ABS, respectively[17]). As a result upon solidification of blends, iPP phase contracts more than the dispersed ABS resulting into tightly embedded ABS in iPP matrix imparting higher impact strength which is also discussed in section 3.4.1.f.

The addition of 2.5 to 5.0 phr HPP-g-STY-MMA graft copolymer as a compatibilizer to 90/10 % iPP/ABS binary blend resulted into higher impact strength, because of the finer and homogineous dispersion and distribution of ABS as an inclusions in iPP matrix (Fig. 3.2.a), due to decrease in interfacial tension and increase in the interfacial adhesion between two phases. This could lead to greater absorption and uniform distribution of impact energy on the whole matrix. However, increase in concentration of compatibilizer to 7.5 phr, dispersed particles aggloramated resulting into increased size(Table3.3) and breakdown of the stable morphology. As a result impact value decreased at higher level of compatibilization in the iPP/ABS blend system. A similar trend was observed by Sathe, et al.[18] for iPP/Nylon/iPP-g-MAH blends.

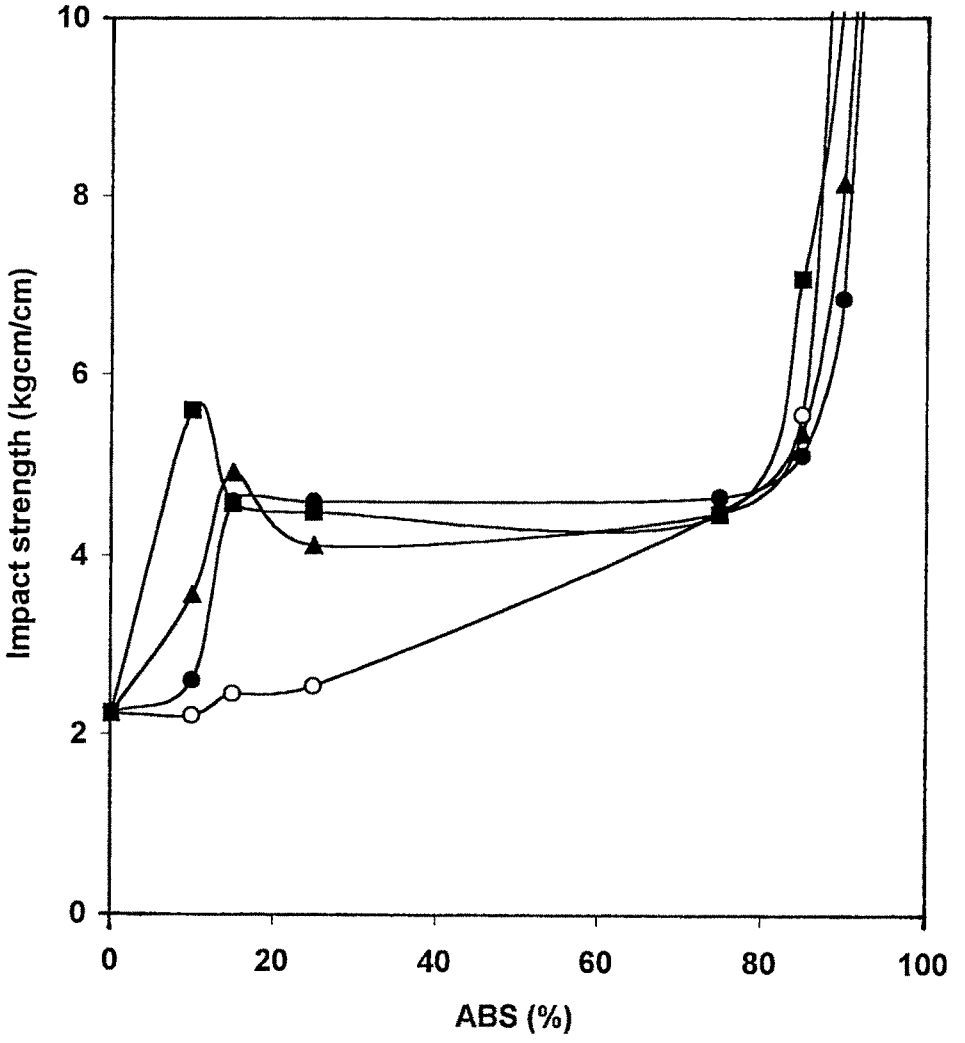

Figure 3.8 : Impact strength of iPP/ABS binary and ternary blends

(o) iPP/ABS binary blends

(■) HPP-g-STY-MMA ternary blend (2.5 phr)

(▲) HPP-g-STY-MMA ternary blend (5.0 phr)

(●) HPP-g-STY-MMA ternary blend (7.5 phr)

3.4.1.c Flexural modulus

Fig. 3.9 illustrates the flexural modulus of iPP/ABS blends. Due to increased adhesion at interface the flexural modulus increases when iPP/ABS blends are compatibilized. The addition of 2.5 to 5.0 phr of compatibilizer gave maximum flexural modulus for the blends containing 10 – 15 % of ABS.

3.4.1.d Melt flow index

The melt flow index provides valuable information about the flow behavior of materials. Fig. 3.10 shows the MFI values of iPP, ABS, iPP/ABS binary and iPP/ABS/HPP-g-STY-MMA ternary blends. From the figure it is observed that MFI values decreased as ABS concentration increased in binary blends. This is because of the lower MFI values of ABS. As the viscosity increases the MFI values decrease. (90/10,%) iPP/ABS blend with 2.5 phr of HPP-g-STY-MMA graft copolymer as a compatibilizer showed lower MFI values than (90/10,%) iPP/ABS binary as well as 90/10/5.0 and 90/10/7.5 (iPP/ABS/HPP-g-STY-MMA) ternary blend system. Incorporation of compatibilizer reduces interfacial tension and it works effectively at the interface. As a result finer dispersion of ABS particles is formed in iPP matrix, leading to stable morphology with resistance to flow behavior. Compatibilizer mainly affects,

- mechanical properties and
- plasticization

In the present system at 2.5 phr level of compatibilizer effect on mechanical properties was more pronounced than on flow properties. This can be attributed to the lower plasticization effect and internal slippages at the two phases resulting into lower MFI. However, at higher compatibilizer level mechanical properties showed decrease and plasticization effect was more, as a result MFI value increased. Shertukda and Kale[19] have also reported the

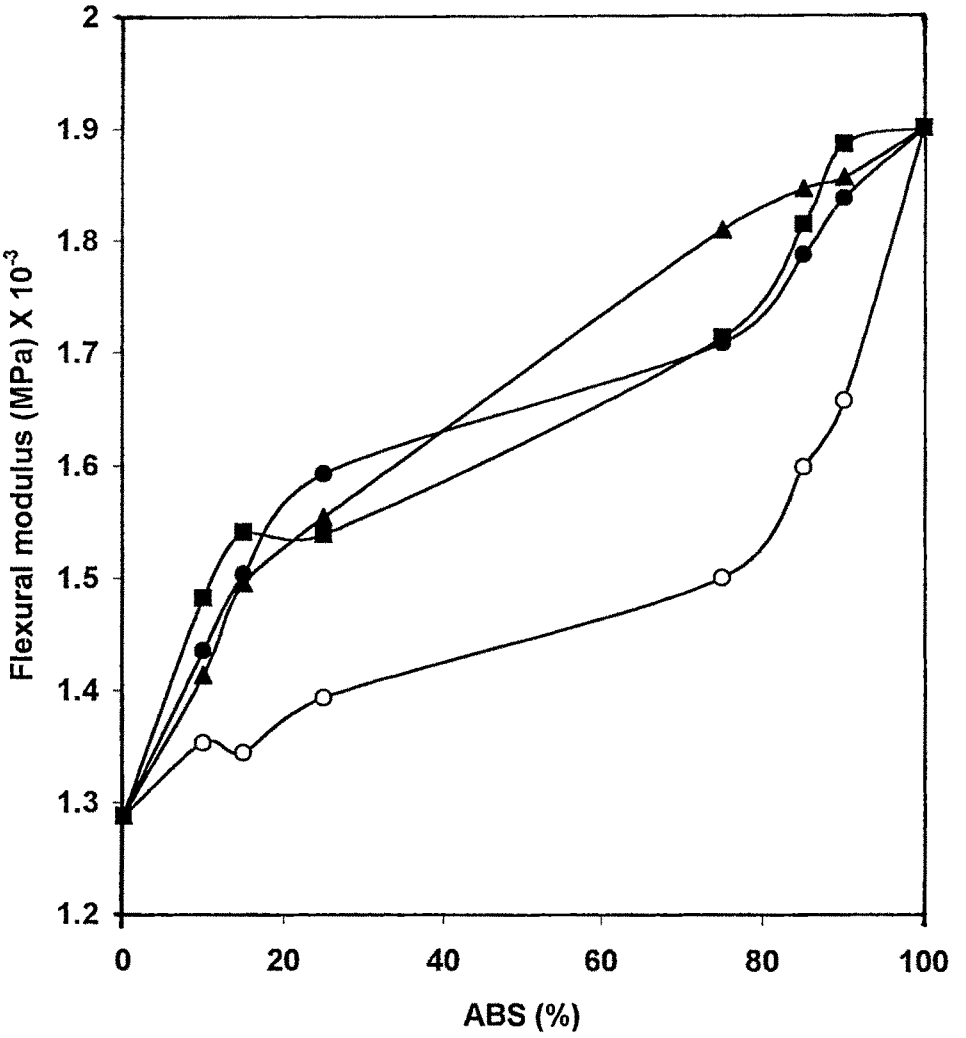

Figure 3.9 : Flexural modulus of iPP/ABS binary and ternary blends

(o) iPP/ABS binary blends

(■) HPP-g-STY-MMA ternary blend (2.5 phr)

(▲) HPP-g-STY-MMA ternary blend (5.0 phr)

(●) HPP-g-STY-MMA ternary blend (7.5 phr)

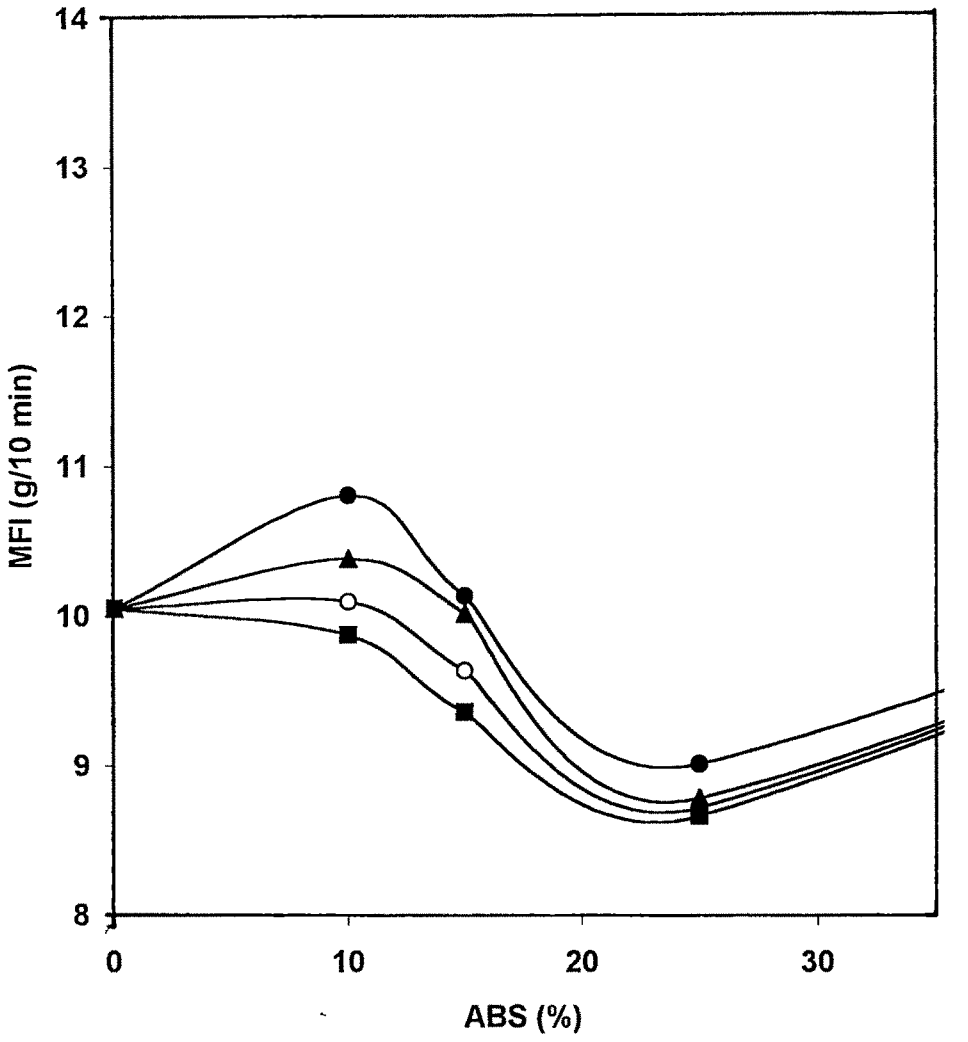

Figure 3.10 : Melt flow index (MFI) of iPP/ABS binary and ternary blends

(o) iPP/ABS binary blends

(■) HPP-g-STY-MMA ternary blend (2.5 phr)

(▲) HPP-g-STY-MMA ternary blend (5.0 phr)

(●) HPP-g-STY-MMA ternary blend (7.5 phr)

higher MFI value than virgin PP for PP/PET blend and suggested that lower viscosity of the blends will improve processability.

3.4.1.e Rheology

The shear viscosity versus shear rate behavior of iPP and ABS and iPP-rich iPP/ABS (90/10, 85/15 & 75/25, %) blends with and without compatibilizer at 220 ^{0}C is shown in Fig. 3.11.a-c. Polypropylene shows somewhat more shear thinning(Non-Newtonian) behavior at higher shear rate. At zero shear the molecules are randomly oriented and highly entangled and therefore exhibit high viscosity and under the application of shear force, the polymer chains orient resulting in the reduction of shear viscosity and exhibiting pseudoplastic behavior. The reduction in viscosity of the blends at higher shear rate is also due to the dispersed domains.

All the results show a very unusual phenomenon where essentially all the viscosity versus shear rate curves for iPP/ABS, (90/10 to 75/25, %) are nearly overlapping. A similar trend was observed by Chang and Chiang[20] for PA-6/PPO/SMA (70/30/2.0 to 10 phr) system. Kozlowski and Bucknall[21] have reported the melt viscosity of the blends becomes closer to that of the corresponding matrix as the shear rate increases particularly at the high shear rates that are typically used for processing, and the melt flow behavior is almost identical for the modified and neat polymers.

The shear viscosity increased in ternary blends as compared to its binary blend (Table 3.4 and Table 3.5). Increase in shear viscosity with increased concentration of compatibilizer can be attributed to better adhesion between the two phases. However, from the results given in Table 3.5 for (75/25, %) iPP/ABS/HPP-g-STY-MMA ternary blend system it is observed that shear viscosity remains constant at all the shear rates and for all the compositions. As a result of this no major change was observed on mechanical properties.

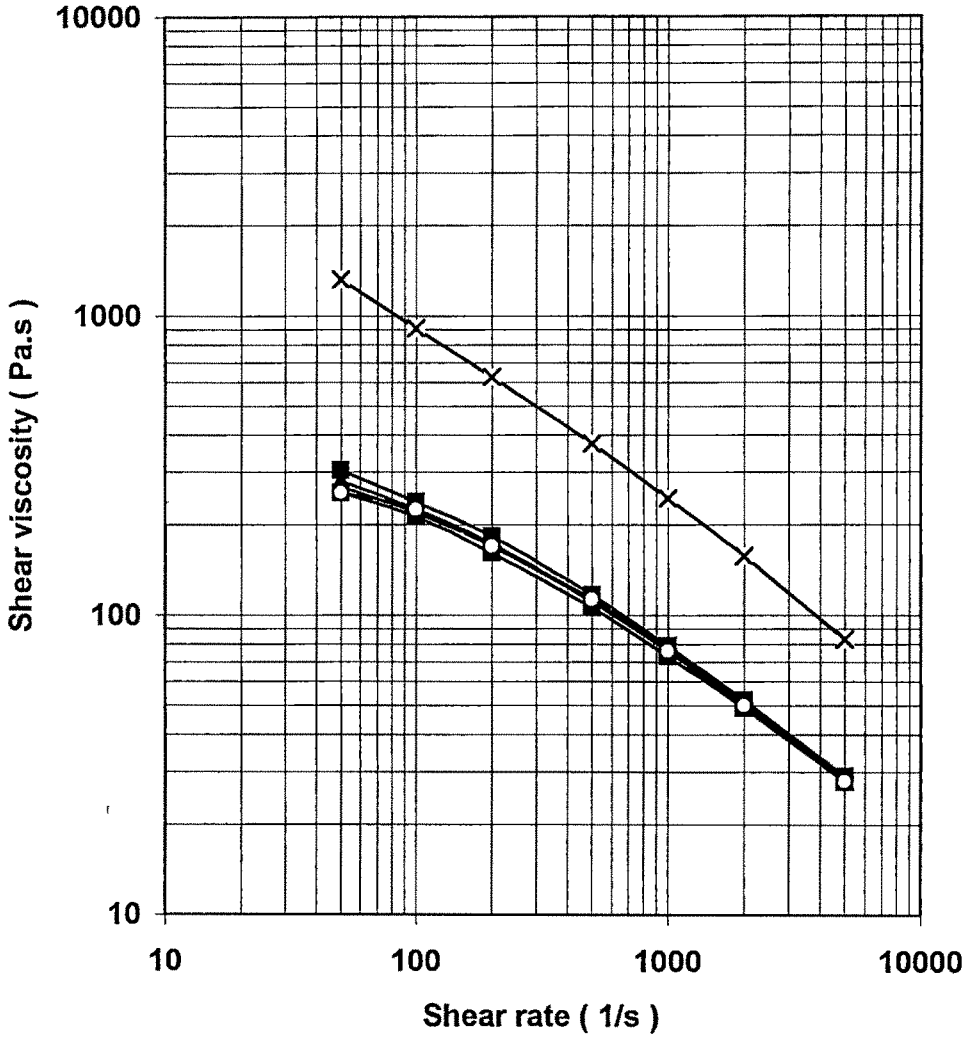

Figure 3.11.a : Shear viscosity of iPP/ABS binary and ternary blends

(X) ABS

(o) iPP

(Δ) iPP/ABS binary blends (90/10)

(■) iPP/ABS/HPP-g-STY-MMA ternary blend (90/10/2.5)

(▲) iPP/ABS/HPP-g-STY-MMA ternary blend (90/10/5.0)

(●) iPP/ABS/HPP-g-STY-MMA ternary blend (90/10/7.5)

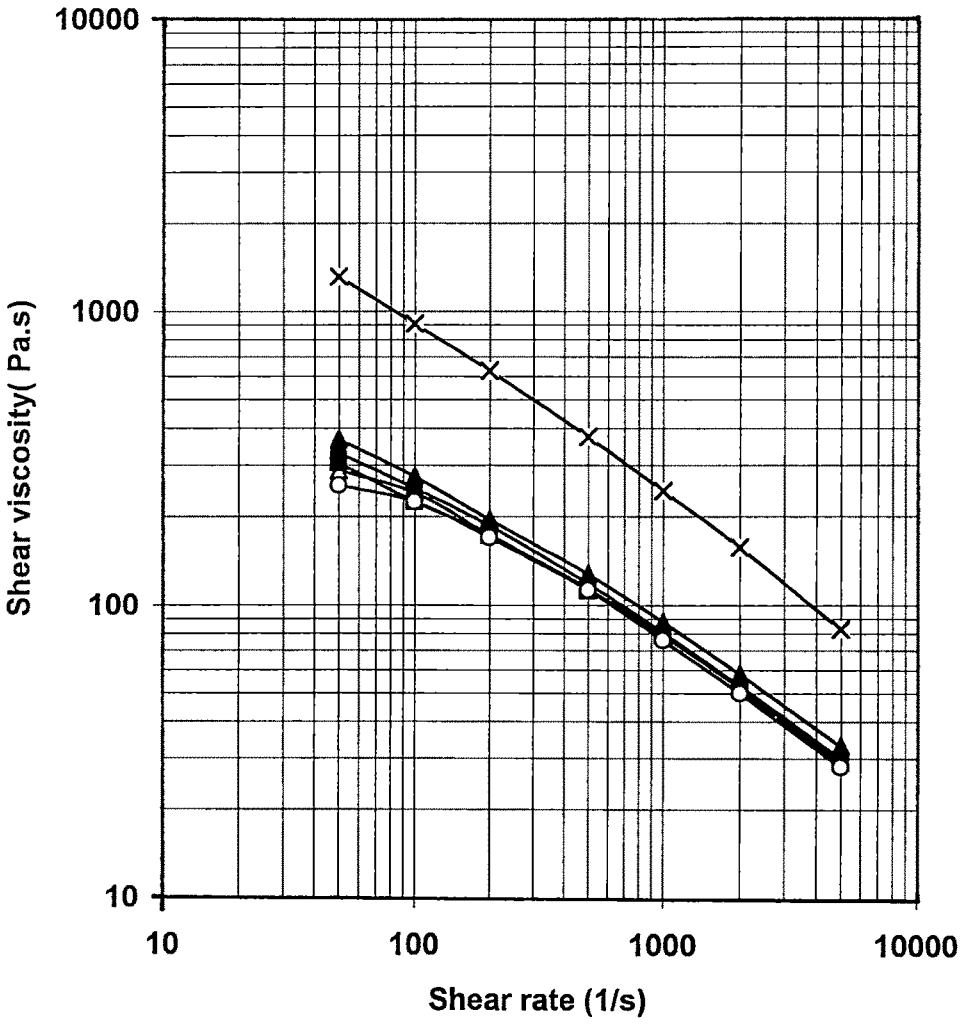

Figure 3.11.b : Shear viscosity of iPP/ABS binary and ternary blends

(X) ABS

(o) iPP

(Δ) iPP/ABS binary blends (85/15)

(■) iPP/ABS/HPP-g-STY-MMA ternary blend (85/15/2.5)

(▲) iPP/ABS/HPP-g-STY-MMA ternary blend (85/15/5.0)

(●) iPP/ABS/HPP-g-STY-MMA ternary blend (85/15/7.5)

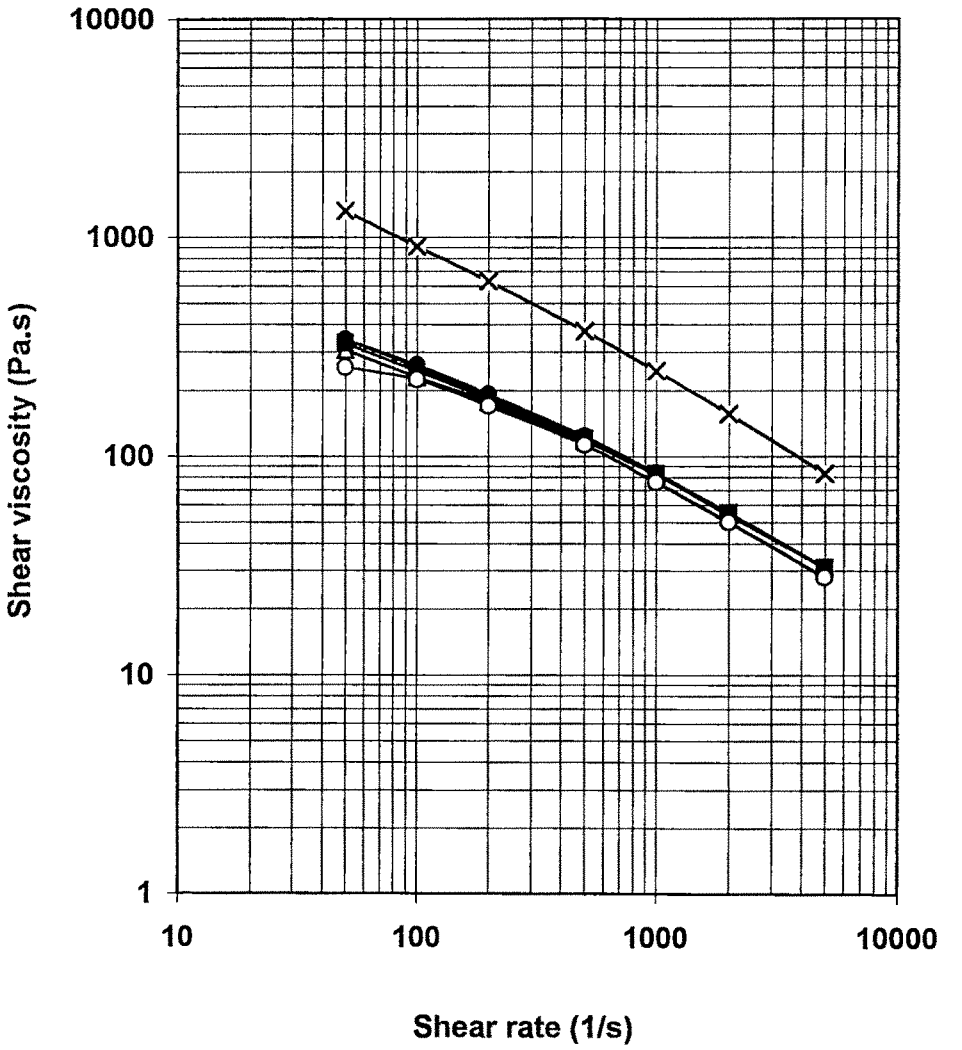

Figure 3.11.c : Shear viscosity of iPP/ABS binary and ternary blends

(X) ABS

(o) iPP

(Δ) iPP/ABS binary blends (75/25)

(■) iPP/ABS/HPP-g-STY-MMA ternary blend (75/25/2.5)

(▲) iPP/ABS/HPP-g-STY-MMA ternary blend (75/25/5.0)

(●) iPP/ABS/HPP-g-STY-MMA ternary blend (75/25/7.5)

Table 3.4 : Shear viscosity for iPP, ABS and iPP/ABS binary blend system at 220 ^{0}C

Shear Rate (1/s)	Shear viscosity(Pa.s)				
	iPP	ABS	iPP/ABS (90/10, %)	iPP/ABS (85/15, %)	iPP/ABS (75/25, %)
50	256	1318	252	268	305
100	225	909	219	228	231
200	170	626	170	174	177
500	113	374	111	113	117
1000	76	245	76	79	82
2000	50	157	51	53	55
5000	28	83	29	30	31

Table 3.5 : Shear viscosity for iPP, ABS and iPP/ABS/HPP-g-STY-MMA ternary blend system at 220 ^{0}C

Shear Rate (1/s)	Shear viscosity(Pa.s)								
	iPP/ABS/HPP-g-STY-MMA system								
	iPP/ABS (90/10 ,%)			iPP/ABS (85/15, %)			iPP/ABS (75/25,%)		
	2.5 phr	5.0 phr	7.5 phr	2.5 phr	5.0 phr	7.5 phr	2.5 phr	5.0 phr	7.5 phr
50	256	280	305	305	329	365	329	341	341
100	213	225	238	225	250	274	245	256	262
200	161	173	183	173	186	195	183	189	192
500	73	112	117	114	119	128	120	120	123
1000	73	77	79	79	81	88	83	83	84
2000	49	51	52	52	53	58	55	54	55
5000	28	28	29	29	30	33	31	31	31

3.4.1.f Mathematical modeling

In Fig. 3.12 the tensile modulus values calculated from the various theoretical models discussed earlier in section 3.2 along with experimental values for iPP/ABS binary and iPP/ABS/HPP-g-STY-MMA (2.5, 5.0 & 7.5 phr) blends are presented. The calculated tensile modulus values were compared with those obtained experimentally. It was observed that Kerner's model for loosely bound inclusions shows considerable negative deviation for binary as well as ternary blends. This implies that the discrete ABS and/or iPP phase is not loosely bound with matrix and some adhesive forces exist between iPP and ABS, which are likely to originate from the stiffening effect, which can be attributed to the higher coefficient of thermal expansion of PP as compared to ABS (1.7×10^{-4} k^{-1} and 0.8×10^{-4} k^{-1} for PP and ABS respectively[17]). As a result upon solidification of blends, iPP–phase contracts more than the dispersed ABS resulting into tightly embedded ABS in iPP matrix imparting increased tensile modulus even in binary blends. However, this effect was observed more when compatibilizer was added. In addition to the stiffening effect the factor further responsible for higher tensile modulus in compatibilized blends is increased homogeneity and finer dispersion observed in ternary blends.

Neilsen's model predicts tensile modulus on the basis of ϕ_{max} values. The ϕ_{max} values were adjusted in such a way that theoretically calculated modulus data matches with the experimentally obtained one. The ϕ_{max} values calculated for adjusting the theoretical values of tensile modulus with experimental data are given in Table 3.6. It was observed that with increased content of ABS, ϕ_{max} values go on increasing, indicating decrease in the volume of the interface, which is immobilized by the discrete phase in the blends. The reciprocal of ϕ_{max} can be considered as an interaction parameter, which is proportional to $(R + \Delta R)^3$, where R is the radius of the inclusion and ΔR is the depth of interface that is immobilized by the inclusion. From Table 3.6, it can be observed that smaller ϕ_{max} value

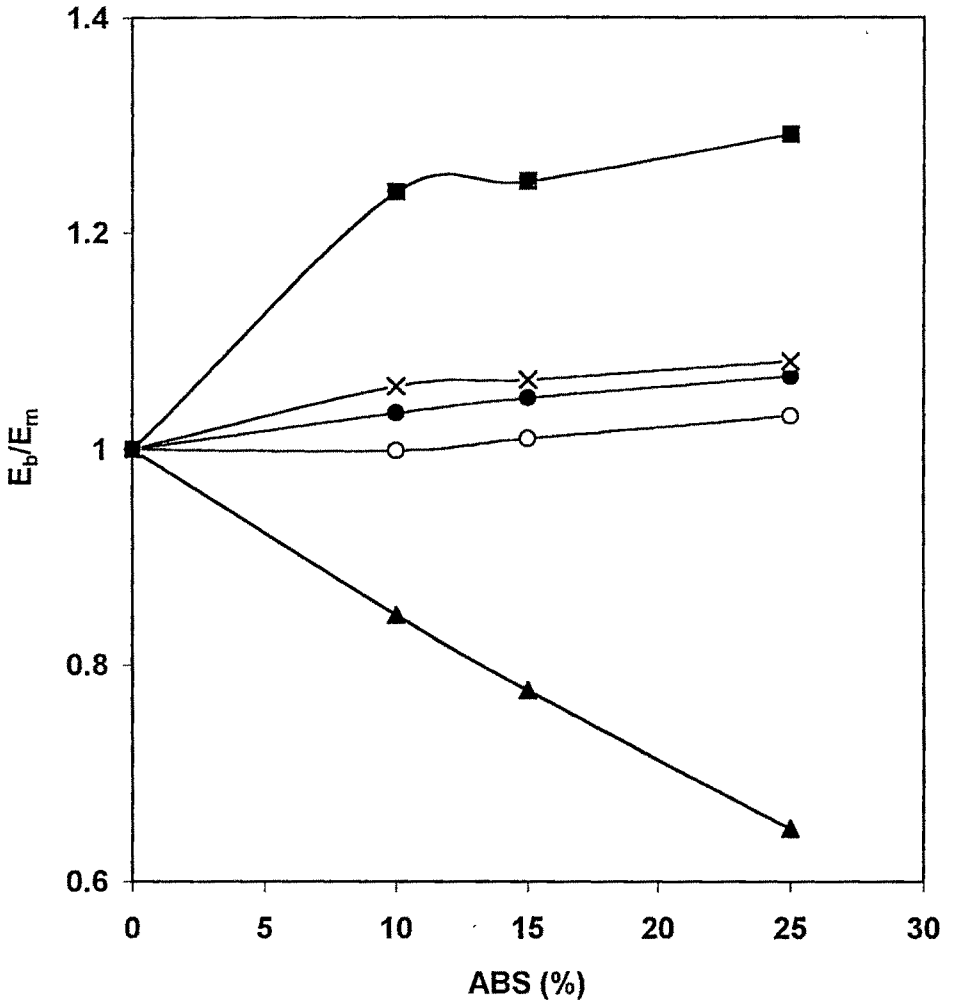

Figure 3.12 : Theoretical models for the tensile modulus of iPP/ABS binary and ternary blends

(●) Kerner's model for perfectly bound inclusion

(▲) Kerner's model for loosely bound inclusion

(X) Neilsen's model for rubber dispersed in rigid matrix

(o) iPP/ABS blends experimental values

(■) iPP/ABS/HPP-g-STY-MMA(2.5 phr) blends experimental values

indicates a larger volume at interface, which is immobilized by the dispersed phase in the blends. The results obtained from SE-micrographs for particle size of the binary/ternary blends (Table 3.3), show that with increasing ABS content in blends, the dispersed particle size increases which supports the observed increase in the $\phi_{max.}$ (Table 3.6).

Table 3.6 : Adjusted ϕ_{max} values for iPP/ABS/HPP-g-STY-MMA system

ABS (%)	ϕ_{max} for iPP/ABS/HPP-g-STY-MMA system			
	HPP-g-STY-MMA 0 (phr)	HPP-g-STY-MMA 2.5(phr)	HPP-g-STY-MMA 5.0(phr)	HPP-g-STY-MMA 7.5(phr)
10	0.45	0.35	0.39	0.44
15	0.69	0.43	0.49	0.52
25	0.75	0.63	0.64	0.67

3.4.2 iPP-g-methacrylic acid (iPP-g-MAA) as a compatibilizer for iPP/ABS blends

The synthesis and characterization of iPP-g-MAA is discussed in Chapter 2. Grafting of methacrylic acid onto polypropylene through solution polymerization was resulted into 6.5% of grafting. In this section the potential of iPP-g-MAA as an interfacial agent (compatibilizer) for iPP/ABS blends is examined.

3.4.2.a Morphology

Scanning electron micrographs of room temperature fractured iPP/ABS binary blends are shown in Fig. 3.1(a,b) in section 3.4.1.a. In binary blends smooth surface between two phases indicates no adhesion between matrix and inclusion. This indicates incompatibility of the phases. The particle size of the ABS as an inclusion in iPP matrix was observed to increase with

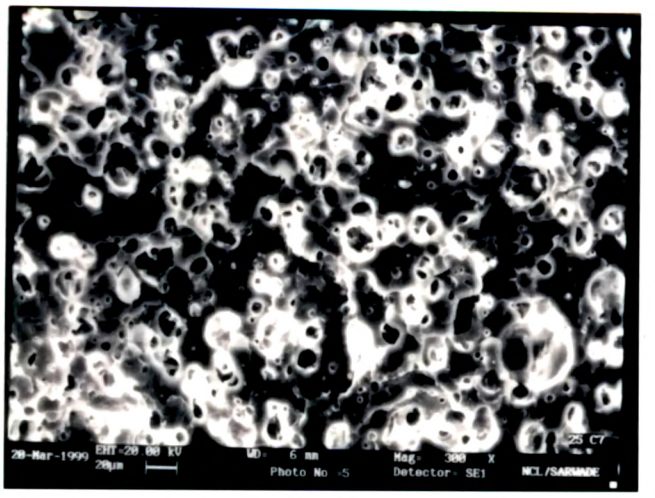

a

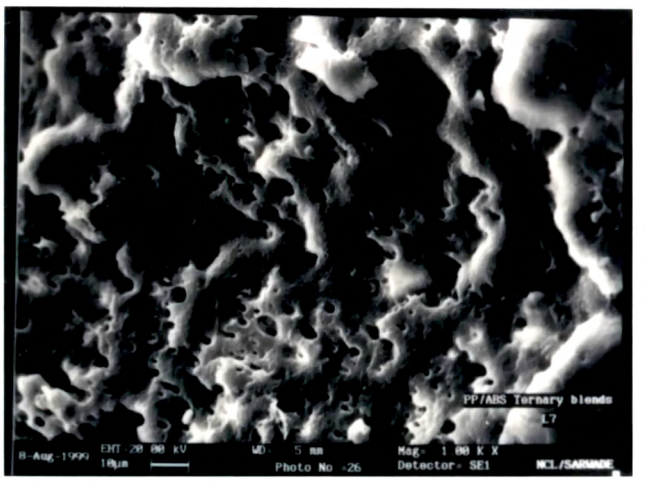

b

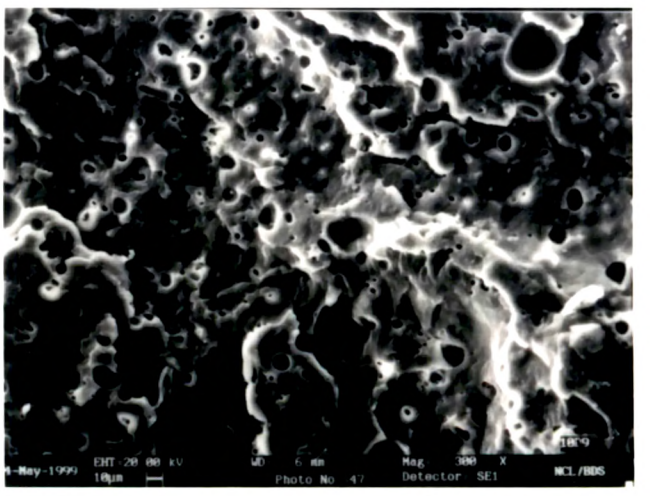

c

Figure 3.13 :SE micrographs of impact fractured surface of iPP/ABS/iPP-g-MAA blends after extraction of ABS in MEK

a : 90/10/2.5 **b** : 90/10/5.0 **c** : 90/10/7.5 iPP/ABS/iPP-g-MAA

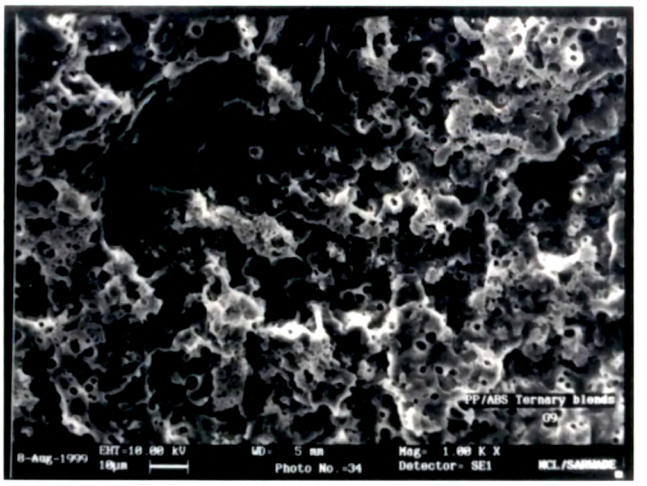

a

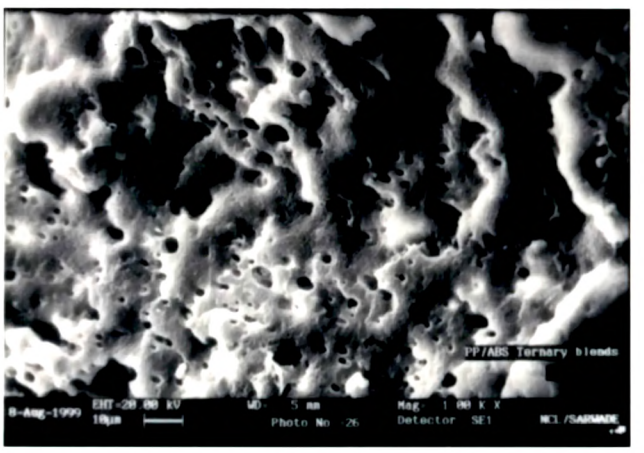

b

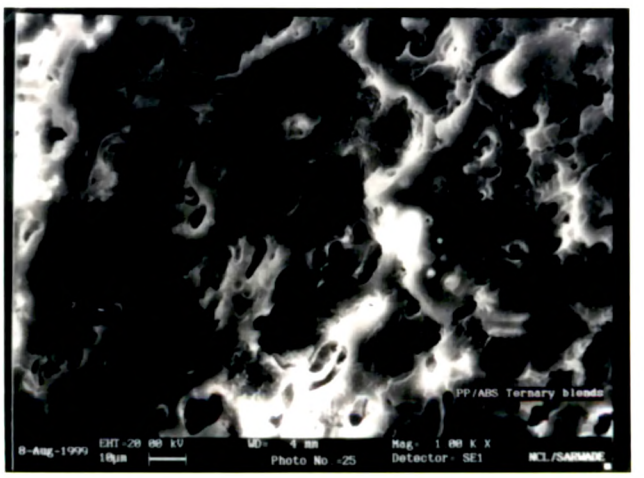

c

Figure 3.14 :SE micrographs of impact fractured surface of iPP/ABS/iPP-g-MAA blends after extraction of ABS in MEK

a : 75/25/2.5 **b** : 75/25/5.0 **c** : 75/25/7.5 iPP/ABS/iPPg-MAA

Table 3.7 : Particle size and polydispersity index(PDI) for iPP/ABS/iPP-g-MAA system

Blend composition iPP/ABS/ iPP-g-MAA* (%)	$\overline{Dn}$(μm)	$\overline{Dw}$(μm)	PDI
90/10/0	2.80	2.28	0.81
90/10/2.5	1.93	2.16	1.12
90/10/5.0	2.18	2.76	1.27
90/10/7.5	2.63	2.93	1.11
75/25/0	5.0	5.78	1.15
75/25/2.5	3.28	3.65	1.11
75/25/5.0	4.19	5.55	1.32
75/25/7.5	4.65	4.51	0.97

* iPP-g-MAA copolymer was added as a compatibilizer in parts per hundred of resin (phr).

increasing concentration of ABS in binary blends. The particle size was observed to increase from 2.80 μm to 5.0 μm for the 90/10 to 75/25 % iPP/ABS blend composition (Table 3.7). Compatibilization of 90/10 % iPP/ABS binary blends with iPP-g-methacrylic acid as a compatibilizer resulted into particles of size 1.93 μm whereas in the blends containing 25 % of ABS the particle size was observed to be 3.28 μm [Fig. 3.13.a and Fig. 3.14.a and Table 3.7]. The size of the dispersed phase particles in the ternary blends was observed to be smaller than that in corresponding binary blends. Addition of 2.5 phr of iPP-g-methacrylic acid to binary blends decrease the particle size and increases the adhesion between matrix and inclusion. Increase in concentration of compatibilizer from 2.5 phr to 7.5 phr will break the stable interface, due to higher lubrication effect and increase the flow behavior as discussed in section 3.4.1.d.

Number average diameter $\overline{D}_n$, weight average diameter $\overline{D}_w$ and polydispersity index(PDI) were determined as per procedure discussed in section 3.3.3.a. The results are given in Table 3.7.

3.4.2.b Tensile properties

Typical stress-strain curves for iPP, ABS, iPP/ABS binary and iPP/ABS/iPP-g-MAA ternary blends with 2.5 to 7.5 phr of compatibilizer are given in Fig. 3.15. The trend observed was similar to that observed for iPP/ABS/HPP-g-STY-MMA system. From the results it can be inferred that on addition of ABS in iPP matrix the ductility of blend decreases and brittleness increases. Incorporation of compatibilizer (iPP-g-MMA) developes a sort of adhesion between two phases imparting toughness to the material.

In Fig. 3.16 and Fig. 3.17, the dependence of the tensile strength and tensile modulus on the blend composition is given in Table 3.2. Due to the lower modulus of iPP the tensile modulus of all binary and ternary blends

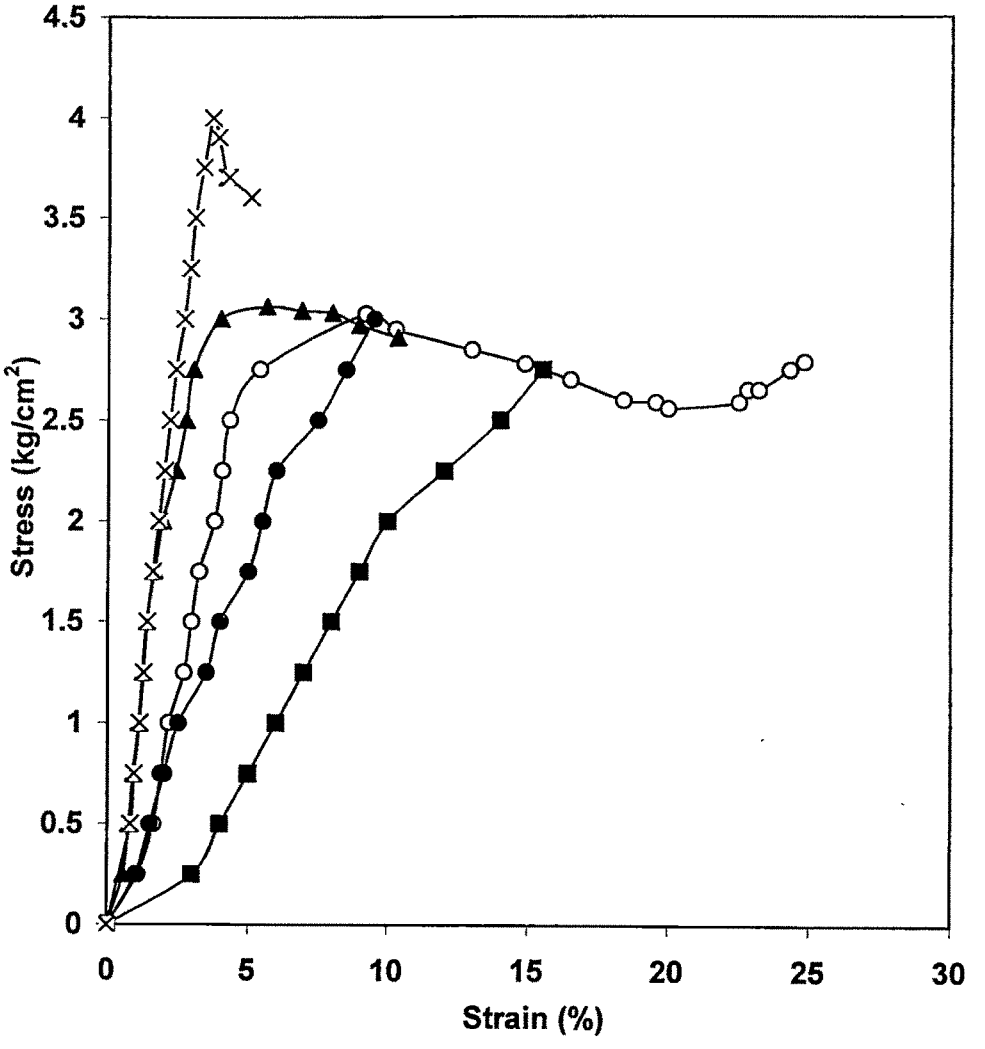

Figure 3.15 : Stress-strain dependence of iPP, ABS and iPP/ABS binary and ternary blend

(X) ABS

(o) iPP

(●) 90/10 iPP/ABS

(■) 75/25 iPP/ABS

(▲) 90/10/2.5 phr iPP/ABS/iPP-g-MAA

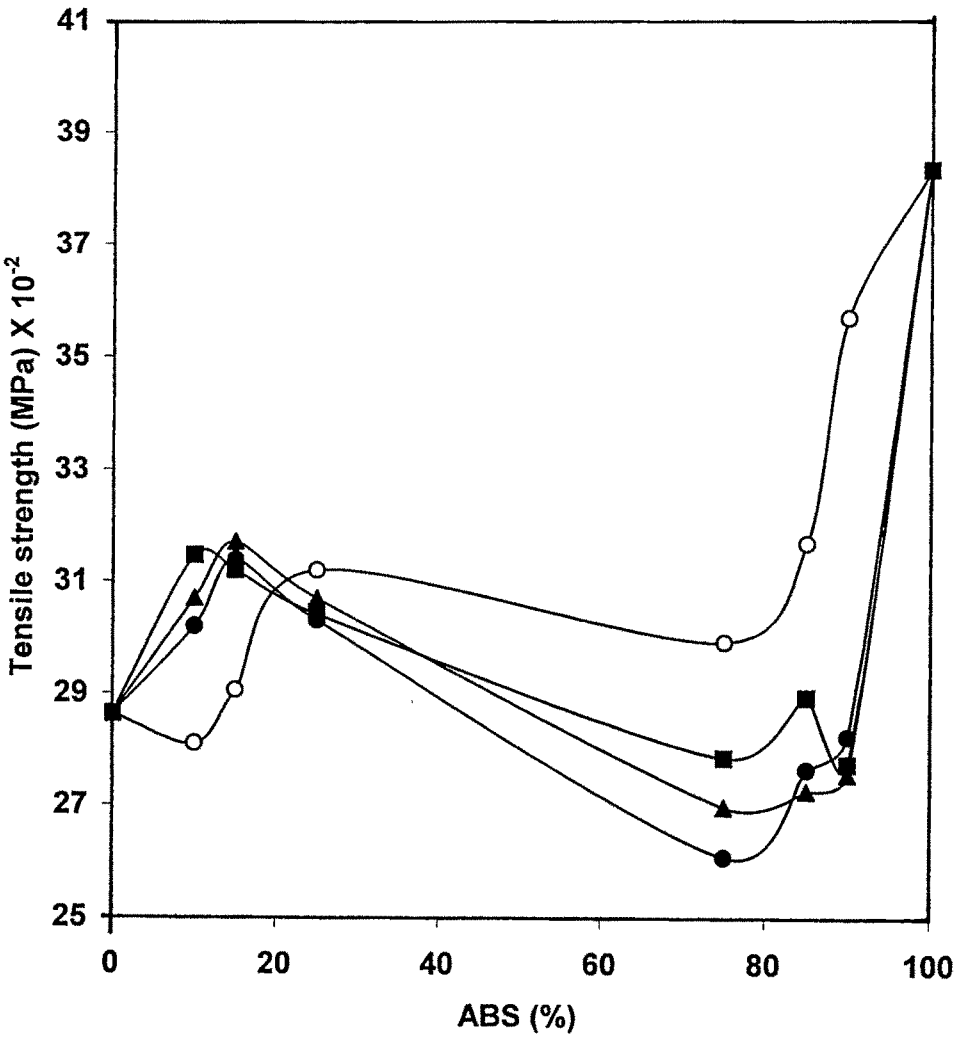

Figure 3.16 : Tensile strength of iPP/ABS binary and ternary blends

(o) iPP/ABS binary blends

(■) iPP-g-MAA ternary blend (2.5 phr)

(▲) iPP-g-MAA ternary blend (5.0 phr)

(●) iPP-g-MAA ternary blend (7.5 phr)

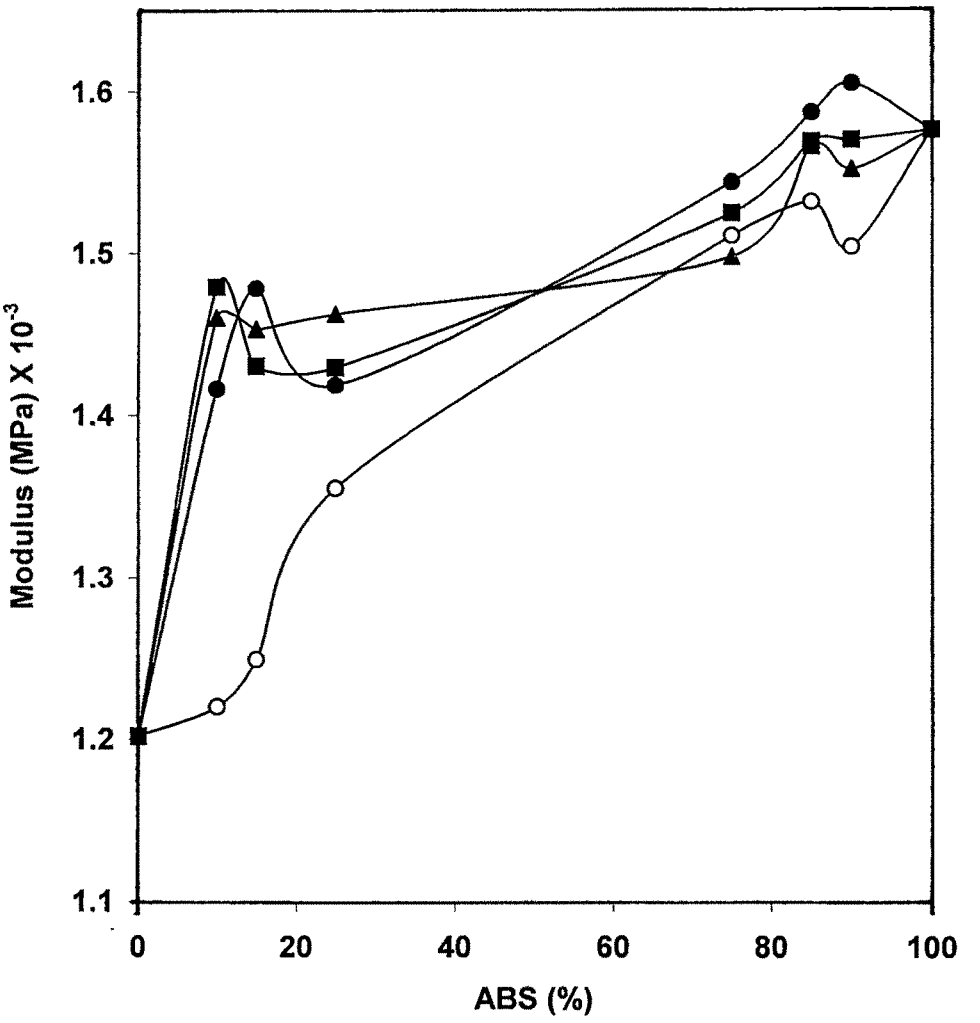

Figure 3.17 : Tensile modulus of iPP/ABS binary and ternary blends

(o) iPP/ABS binary blends

(■) iPP-g-MAA ternary blend (2.5 phr)

(▲) iPP-g-MAA ternary blend (5.0 phr)

(●) iPP-g-MAA ternary blend (7.5 phr)

were observed to be lower than that of ABS. Incorporation of iPP in ABS did not show considerable effect on mechanical properties, whereas incorporation of ABS as an inclusion in iPP matrix showed considerable increase in the mechanical properties such as tensile modulus, tensile strength and flexural modulus of blends. This may be due to the finer and homogeneous dispersion and increased adhesion at the interface. 2.5 to 5.0 phr of compatibilizer was observed to be sufficient to increase the tensile modulus two folds. Higher level of compatibilizer (7.5 phr) decreased both the tensile modulus and tensile strength.

Fig. 3.18 illustrates the % elongation at break for iPP, ABS, iPP/ABS binary and iPP/ABS/iPP-g-methacrylic acid ternary blend system. Sharp decrease in % elongation at break was observed in binary as well as ternary blends on the incorporation of ABS. This shows that crystallinity of iPP decreases. Highest % elongation was observed in (90/10, %) iPP/ABS blends with 2.5 phr of compatibilizer, while in (75/25, %) iPP/ABS blend with 7.5 phr concentration of compatibilizer shows poor elongation properties.

3.4.2.c Impact strength

Fig. 3.19 illustrates the impact strength of iPP/ABS binary and iPP/ABS/iPP-g-MAA ternary blends as a function of blend composition. From the results it is observed that 90/10 % iPP/ABS composition with 2.5 phr of compatibilizer gives good impact properties. The observed higher value of impact strength may be due to the improved homogeneity of the system. SE-micrograph Fig. 3.13.a of 90/10 % iPP/ABS blend with 2.5 phr of compatibilizer shows a good adhesion between two phases. With higher level of compatibilizer (7.5 phr) impact strength was observed to decrease. This is due to the formation of aggregates of compatibilizer in bulk phase after critical concentration of compatibilizer, when excess of the compatibilizer goes to bulk phase in the system and decreases the impact strength.

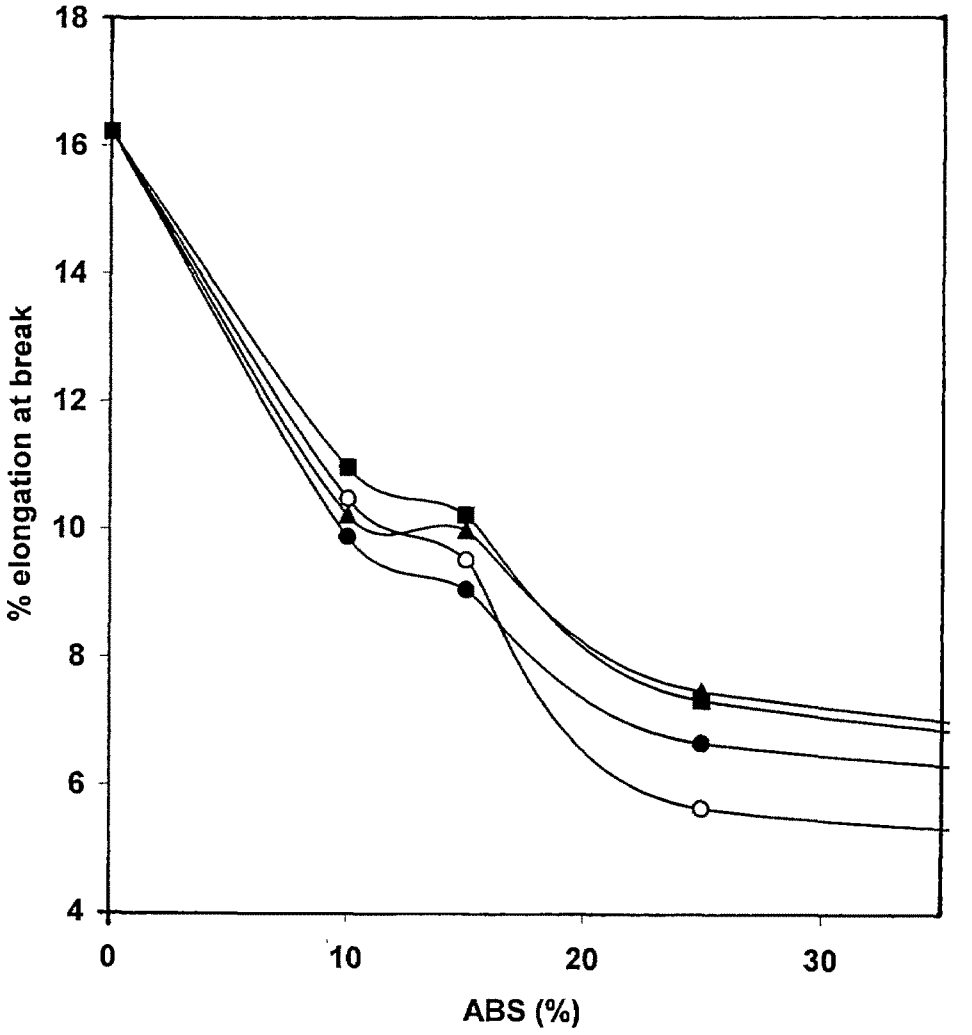

Figure 3.18 : % elongation at break of iPP/ABS binary and ternary blends

(o) iPP/ABS binary blends

(■) iPP-g-MAA ternary blend (2.5 phr)

(▲) iPP-g-MAA ternary blend (5.0 phr)

(●) iPP-g-MAA ternary blend (7.5 phr)

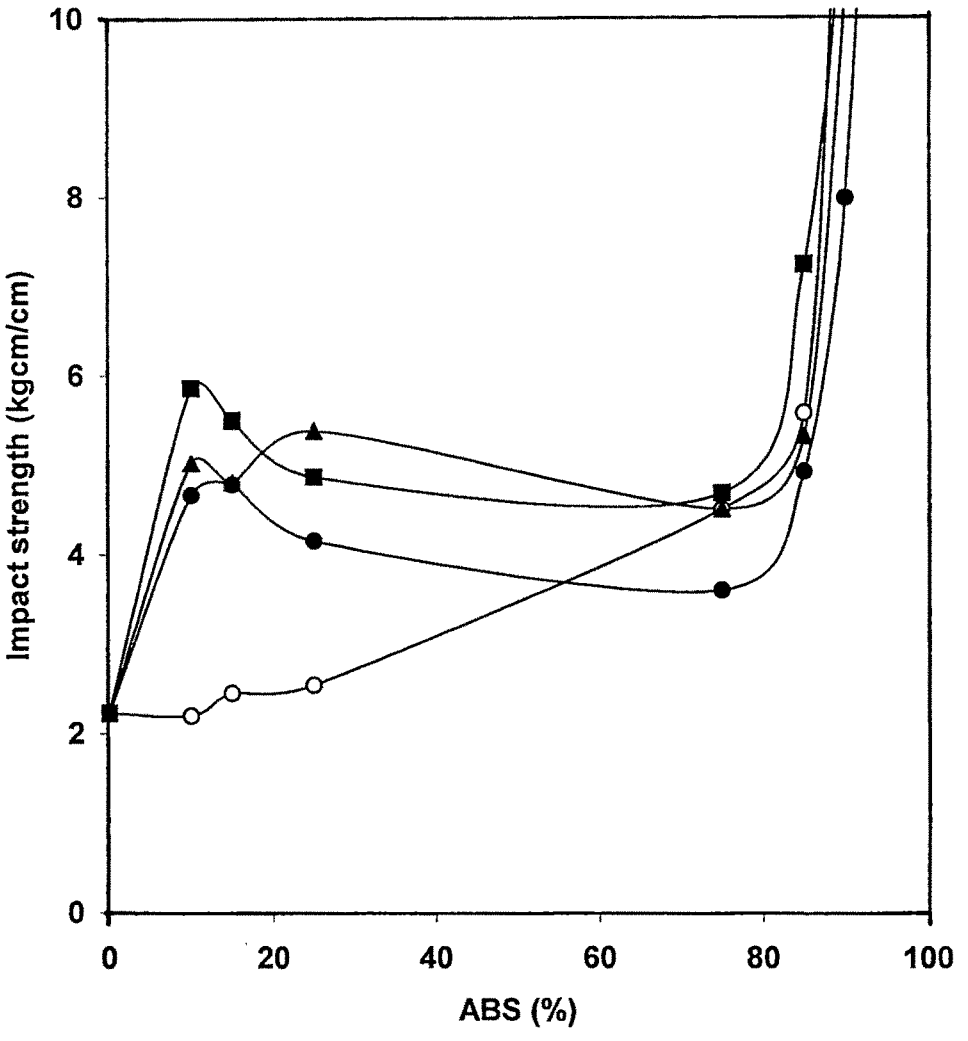

Figure 3.19 : Impact strength of iPP/ABS binary and ternary blends

(o) iPP/ABS binary blends

(■) iPP-g-MAA ternary blend (2.5 phr)

(▲) iPP-g-MAA ternary blend (5.0 phr)

(●) iPP-g-MAA ternary blend (7.5 phr)

3.4.2.c Flexural modulus

Fig. 3.20 illustrates the flexural modulus of iPP/ABS binary and iPP/ABS/iPP-g-MAA ternary blend system. From the results it is observed that flexural modulus in binary and / or in ternary blends was observed to increase with ABS concentration due to the higher modulus values of ABS. Ternary blends showed higher flexural modulus compared to corresponding binary blends. From Fig. 3.20 it is observed that 5.0 phr of compatibilizer gave best results. With increase in concentration of compatibilizer from 5.0 to 7.5 phr flexural modulus was observed to decrease.

3.4.2.d Melt flow index

Fig. 3.21 shows the MFI values of iPP, ABS, iPP/ABS binary and iPP/ABS/iPP-g-methaacrylic acid blend systems. From the results it is found that MFI decreases with increase of ABS concentration in binary blends. iPP/ABS (90/10, %) with 2.5 phr of iPP-g-MAA copolymer as a compatibilizer shows lower MFI values, due to the adhesion between two phases and finer and homogeneous dispersion of inclusion in matrix. Increase in melt flow with increased concentration of compatibilizer can be attributed to the lubrication action of it resulting into decreased resistance and increased flow. Similar trend was also observed in earlier iPP/ABS/HPP-g-STY-MMA system.

3.4.2.e Rheology

The shear viscosity versus shear rate behavior of pure component and iPP-rich (90/10, 85/15 and 75/25 %) blends with 2.5 phr to 7.5 phr of compatibilizer for iPP/ABS/iPP-g-MAA system at 220 ^{0}C is shown in Fig. 3.22.a-c. The detailed discussion on flow behavior of the material in presence and in absence of compatibilizer is given in section 3.4.1.e. This system follows the opposite trend than iPP/ABS/HPP-g-STY-MMA system. All ternary blends show lower shear viscosity than corresponding binary blends and with

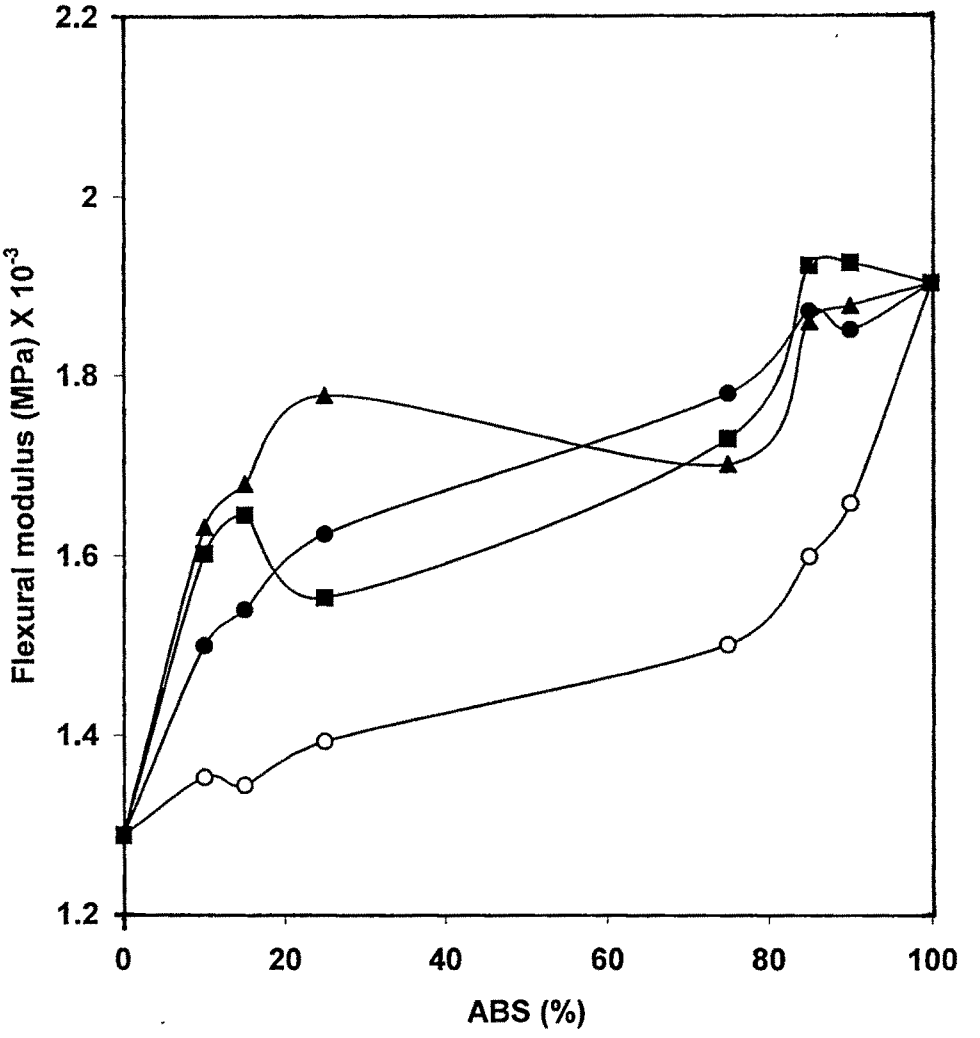

Figure 3.20 : Flexural Modulus of iPP/ABS binary and ternary blends

(o) iPP/ABS binary blends

(■) iPP-g-MAA ternary blend (2.5 phr)

(▲) iPP-g-MAA ternary blend (5.0 phr)

(●) iPP-g-MAA ternary blend (7.5 phr)

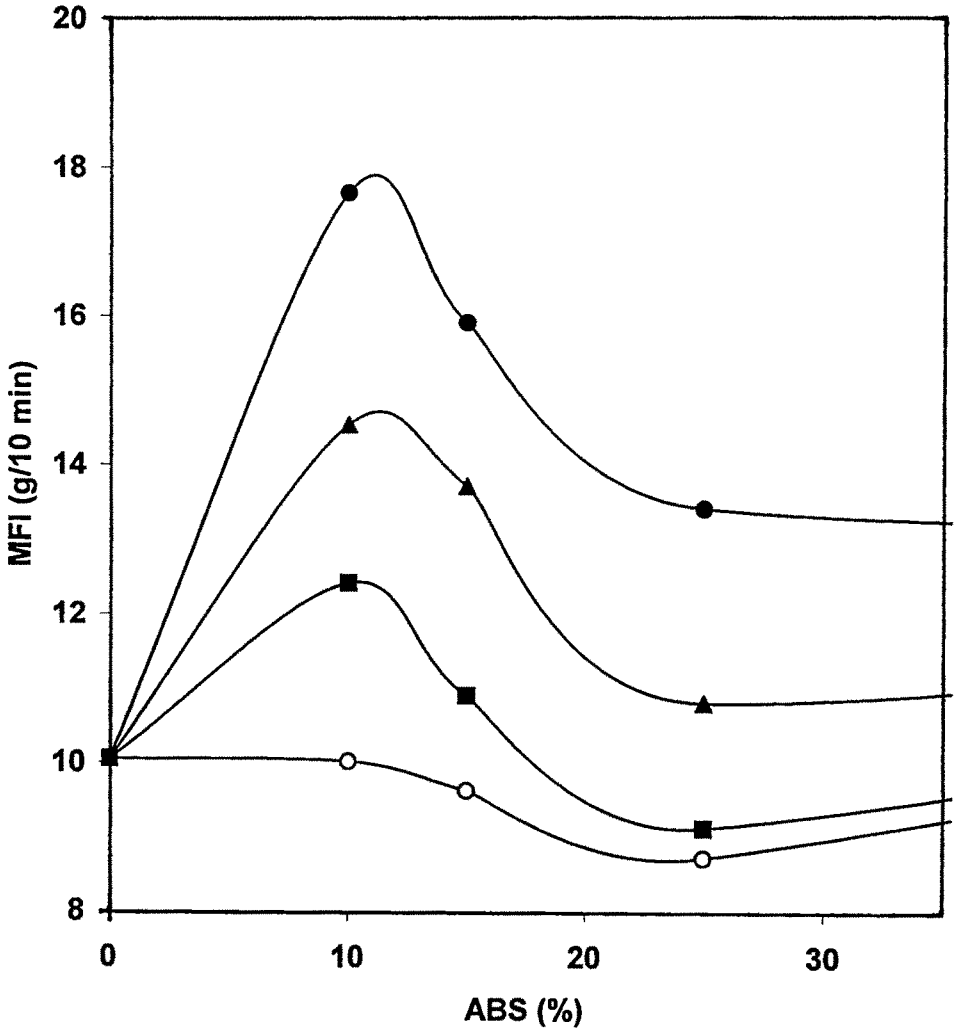

Figure 3.21 : Melt flow index(MFI) of iPP/ABS binary and ternary blends

(o) iPP/ABS binary blends

(■) iPP-g-MAA ternary blend (2.5 phr)

(▲) iPP-g-MAA ternary blend (5.0 phr)

(●) iPP-g-MAA ternary blend (7.5 phr)

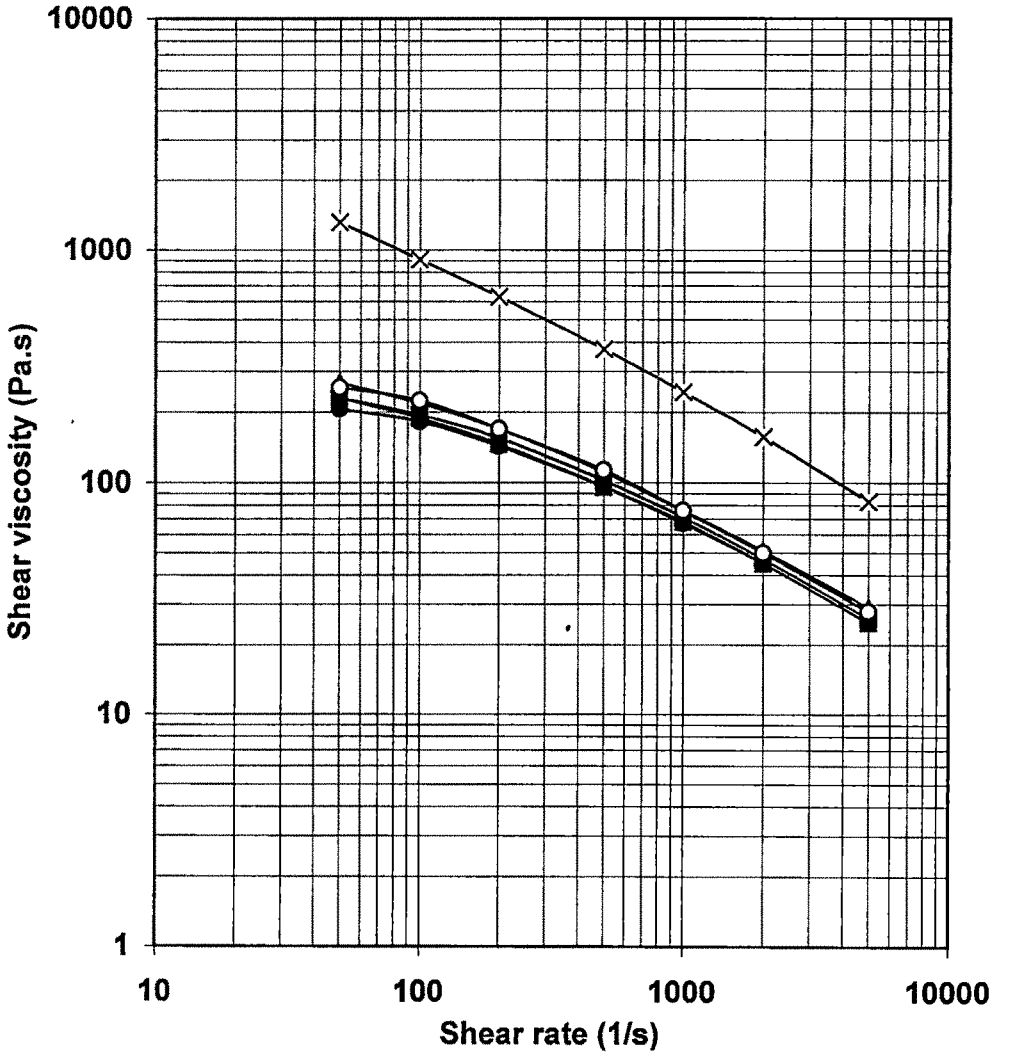

Figure 3.22.a : Shear viscosity of iPP/ABS binary and ternary blends

(X) ABS

(o) iPP

(Δ) iPP/ABS binary blend (90/10)

(■) iPP/ABS/PP-g-MAA ternary blend (90/10/2.5)

(▲) iPP/ABS/PP-g-MAA ternary blend (90/10/5.0)

(●) iPP/ABS/PP-g-MAA ternary blend (90/10/7.5)

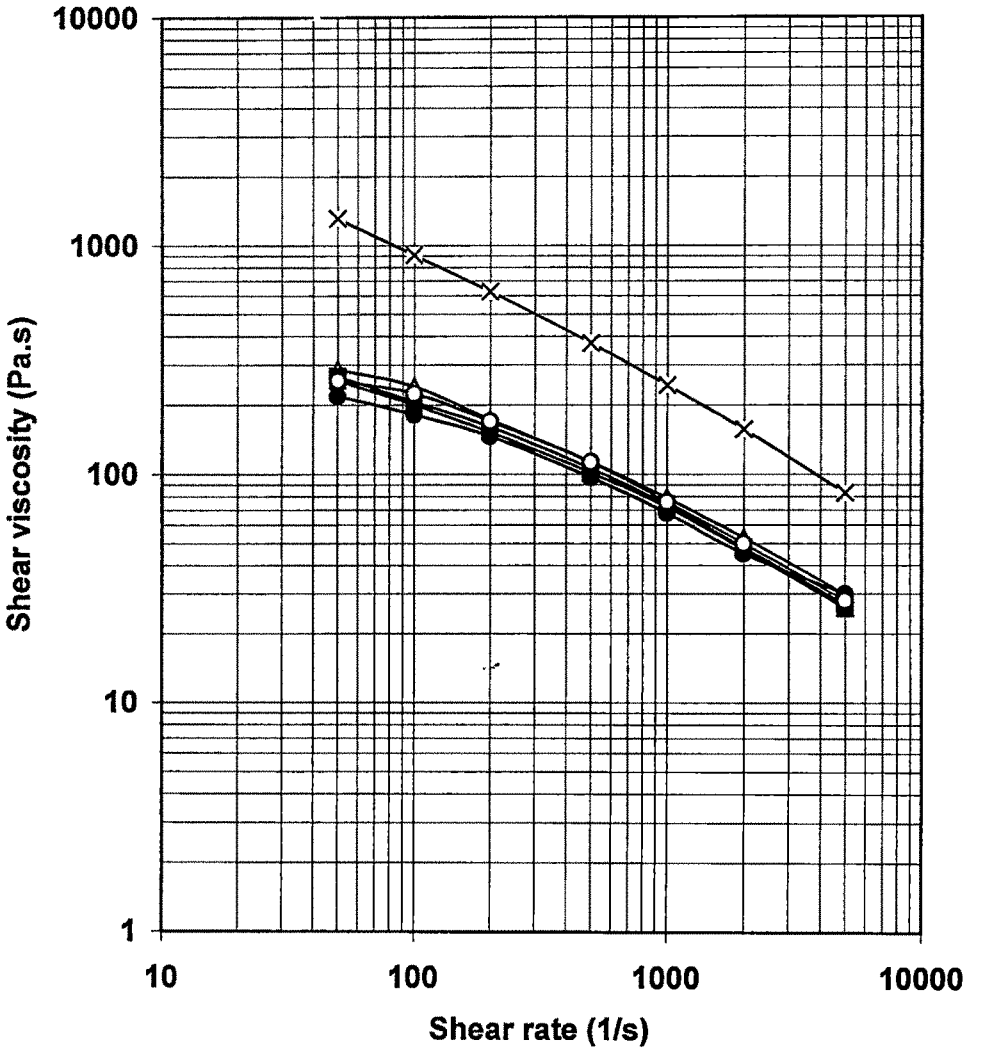

Figure 3.22.b : Shear viscosity of iPP/ABS binary and ternary blends

(X) ABS

(O) iPP

(Δ) iPP/ABS binary blend (85/15)

(■) iPP/ABS/PP-g-MAA ternary blend (85/15/2.5)

(▲) iPP/ABS/PP-g-MAA ternary blend (85/15/5.0)

(●) iPP/ABS/PP-g-MAA ternary blend (85/15/7.5)

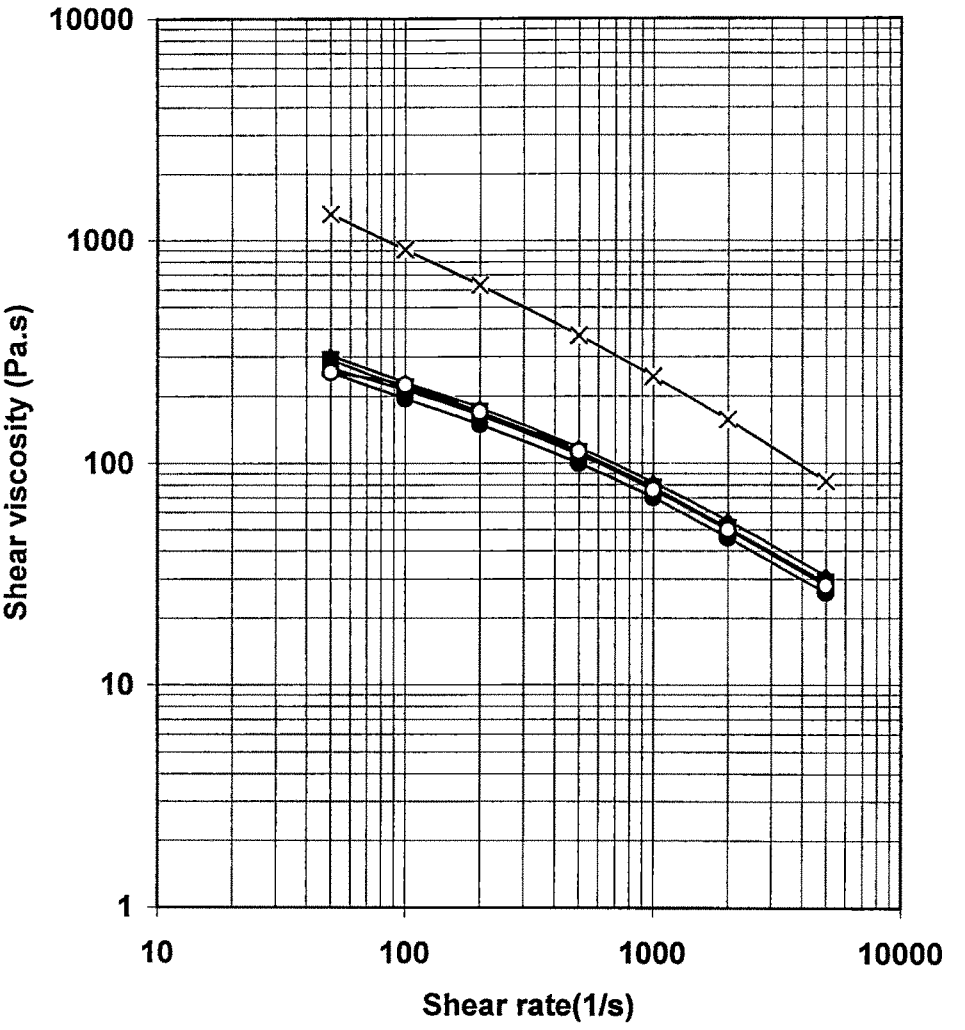

Figure 3.22.c : Shear viscosity of iPP/ABS binary and ternary blends

(X) ABS

(o) iPP

(Δ) iPP/ABS binary blend (75/25)

(■) iPP/ABS/PP-g-MAA ternary blend (75/25/2.5)

(▲) iPP/ABS/PP-g-MAA ternary blend (75/25/5.0)

(●) iPP/ABS/PP-g-MAA ternary blend (75/25/7.5)

Table 3.8 : Shear viscosity for iPP, ABS and iPP/ABS/iPP-g-MAA ternary blend system at 220 ^{0}C

Shear Rate (1/s)	Shear viscosity(Pa.s) iPP/ABS/iPP-g-MAA system								
	iPP/ABS (90/10 ,%)			iPP/ABS (85/15, %)			iPP/ABS (75/25,%)		
	2.5 phr	5.0 phr	7.5 phr	2.5 phr	5.0 phr	7.5 phr	2.5 phr	5.0 phr	7.5 phr
50	231	231	207	268	256	219	292	268	256
100	195	189	182	207	201	182	219	213	195
200	155	146	143	161	152	146	170	164	149
500	102	96	96	106	102	97	112	109	100
1000	71	68	67	74	72	68	78	76	70
2000	47	45	45	48	47	45	51	50	46
5000	26	25	25	27	26	30	29	28	26

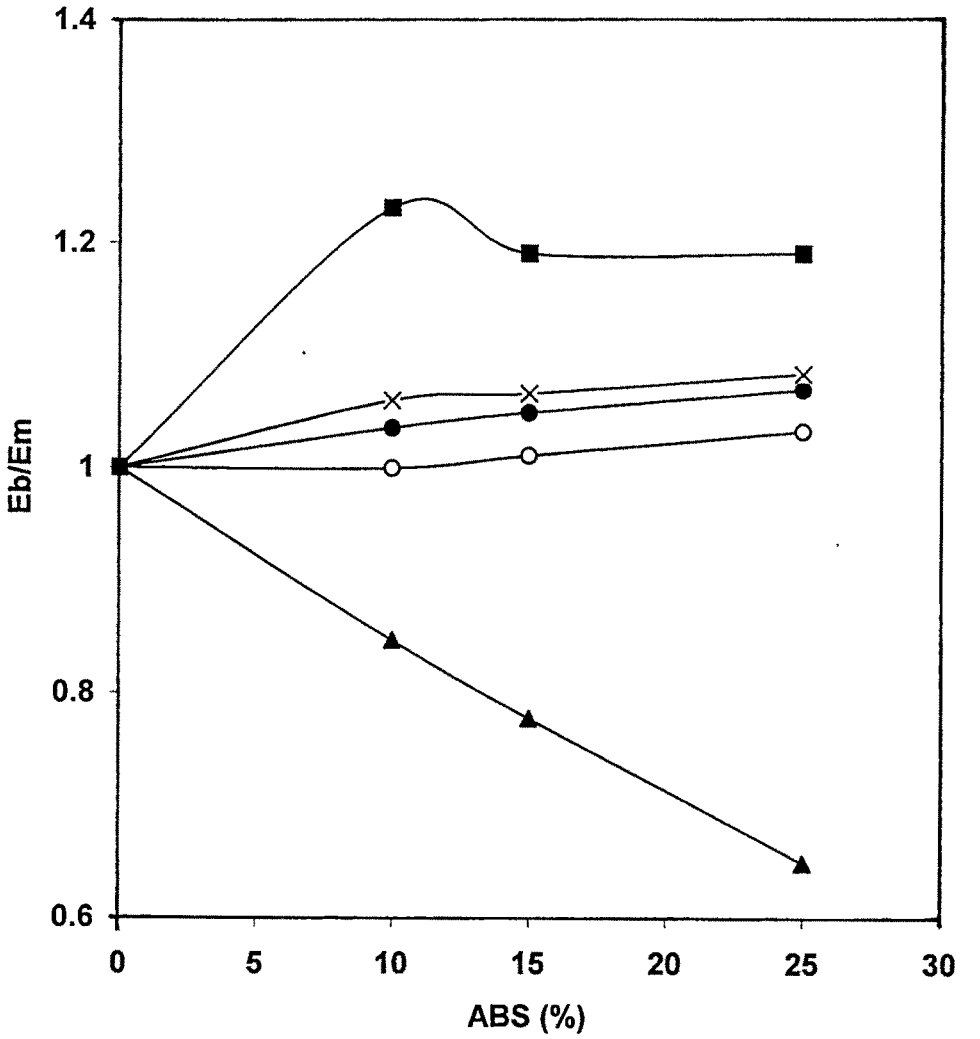

Figure 3.23 : Theoretical models for the tensile modulus of iPP/ABS binary and ternary blends

(●) Kerner's model for perfectly bound inclusion

(▲) Kerner's model for loosely bound inclusion

(X) Neilsen's model for rubber dispersed in rigid matrix

(o) iPP/ABS blends experimental values

(■) iPP/ABS/iPP-g-MAA(2.5 phr) blends experimental values

increase in concentration of compatibilizer shear viscosity still decreases (Table 3.8). Hence, it indicates that higher level of compatibilizer can not stabilize the interface of two polymer, as a result of this mechanical properties were also observed to decrease with high level of compatibilizer.

iPP/ABS 90/10 % blend with 2.5 phr of compatibilizer gave higher shear viscosity than 5.0 and 7.5 phr of compatibilizer. As a result, good mechanical properties were observed for this composition. While in 85/15 % iPP/ABS blends, 2.5 to 5.0 phr of compatibilizer was found to be optimal to obtain better mechanical properties. Percentage elongation was observed to decrease in ternary blends 90/10 % iPP/ABS with 2.5 phr of iPP-g-MAA gave higher elongation than binary as well as corresponding ternary blend with 5.0 and 7.5 phr compatibilizer. This observation clearly supports the rheological characteristics of 90/10 iPP/ABS blends with 25 phr of compatibilizer.

3.4.2.f Mathematical modeling on iPP/ABS/iPP-g-MAA system

To see the validity of the models proposed and discussed earlier in section-3.2, for the prediction of tensile modulus of iPP/ABS binary and iPP/ABS/iPP-g-MAA ternary blend systems, experimentally observed tensile modulus values were compared with those calculated from the various models. From the results given in Fig. 3.23, it is observed that experimental values differ widely from the values observed from the model based on loosely bound inclusions but experimental values show good agreement with the values observed from Kerner's model which is based on perfect adhesion between inclusion and matrix.

3.5 Conclusion

Due to the differences in the nature of the constituents iPP/ABS blends are not compatible with each other. The blends show considerable variations in mechanical and rheological properties, particularly in iPP-rich region upon

addition of 2.5 to 7.5 phr of iPP-g-MAA and HPP-g-STY-MMA copolymer as a compatibilizer.

Following are the major observations

(1) The blends exhibit good tensile and flow behaviour at 10 to 15 % incorporation of ABS in polypropylene.

(2) The experimental data for tensile modulus of the compatibilized ternary blends for both the systems could follow Kerner's model. Electron micrographs of fractured surfaces of blends showed adhesion between the two phases. The ϕ_{max} values obtained through Neilsen's model indicated large and coarse particle formation in binary blends whereas smaller particle formation on compatibilization. The smaller particle size of the dispersed ABS phase at 2.5 phr loading of the compatibilizer and further increase in compatibilizer concentration leading to biggger particles can be attributed to the formation of aggregates of compatibilizer in the bulk phase after exceeding critical concentration of the compatibilizer.

However, iPP/ABS blends are not similar to PP/Nylon-6. ABS itself being a ternary system the proposed models do show difference in character. It can not be overlooked that the observed tensile modulus for the ternary iPP/ABS/iPP-g-STY-MMA or iPP/ABS/iPP-g-MAA blends is higher than that predicted by Kerner's and/or Neilsen's models. This can be attributed to the complex blend system.

(3) The ABS rich blends showed poor mechanical properties and also poor morphology and may not be of commercial use.

(4) Use of HPP-g-STY-MMA as a compatibilizer for iPP/ABS blends showed improvement in izod impact strength, tensile strength, tensile modulus and flow properties. The 2.5 phr level of compatibilizer was observed to be

critical for the improvement in the properties. Kerner's model for perfect adhesion was observed to be applicable only for iPP rich ternary blends. The ϕ_{max} values obtained through Nielsen's model for perfect adhesion also indicate large and coarse particle formation in binary blends whereas smaller particle formation after compatibilization which is also supported through SE photographs.

(5) Higher level of compatibilizer gives internal lubricating effect as a result flow properties are improved.

(6) iPP-g-MAA also showed improvement in izod impact strength, tensile strength, tensile modulus and flow properties of iPP/ABS blends. The 2.5 phr level of concentration of compatibilizer was observed to be critical for the iPP/ABS (90/10 %) blend for the improvement in the properties.

(7) ϕ_{max} values obtained through Nielsen's model for perfect adhesion indicate large and coarse particle formation in binary blends whereas smaller particles formed after compatibilization which was supported by SE photograph and MFI values. Compatibilization of blends resulted into smaller size of dispersed phase (ABS) in iPP-rich blends. The particles were observed to be finer and homogeneous.

(8) iPP/ABS/HPP-g-STY-MMA ternary blend show better performance than iPP/ABS/iPP-g-MAA ternary blends in terms of tensile strength, tensile modulus and % elongation at break.

References

(1) Sternstein, S. S. and Ongchin, L., *Polymer Preprints.*, **10(2),** 1117, (1969).

(2) Kambour, R. P., *Polymer,* **5,** 143, (1964).

(3) Bucknall, C. B. and Smith, R. R., *Polymer.,* **6,** 437, (1965).

(4) Bucknall, C. B., Clayton, D. and Keast, W. E., *J. Mat. Sci.,* **7,**1443, (1972).

(5) Yee, A. F.,, *J. Mat. Sci.,* **12,** 757, (1977).

(6) Hobbs, S. Y. *J. Appl. Phys.,* **48,** 4052, (1977).

(7) Mexwell, M. A. and Yee, A. F., *Polym. Eng. Sci.,* **21,** 205, (1981).

(8) Boggreve, R. J. M., Gaymans, R. J. and Eichenwald, H. M., *Polymer.,* **30,** 78, (1989).

(9) Wu, S., *Polymer.,* **26,** 1855, (1985).

(10) Wu, S., *J. Appl. Polym. Sci.,* **35,** 549, (1988).

(11) Dickie, R. A., *J. Polym. Sci., Polym. Phy. Ed.,* **14,** 2073 (1976).

(12) Kerner, E. H., *Proc. Phys. Soc.,* **69B,** 808 (1950).

(13) Nielsen, L E., *" Mechanical Properties of Polymer and Composite., Marcel Dekker.;"* New York., (1974).

(14) Paul, B., *Trans. Metallurgy. Soc., AIMl,* **218,** 36, (1960).

(15) Masoud, F and Paul, B. R., *Iranian J. of Polym. Sci., and Tech.,* **2,** 2, (1993).

(16) Han, M. S., Lim, B. H., Jung, H. C., Hyun, J. C., Kin, S. R. and Kim, W. N., *Korea-Australia Rgeology J.,* **13(4),** 169, (2001).

(17) Brndrup, J., Emergut, E. H., Ed., Wiley Intersciences., New York., *"Polymer Handbook.,"* (1985)

(18) Sathe, S. N., Devi, S., Rao, G. S. S. and Rao, K. V., *J. Appl. Polym. Sci.,* **61,** 87, (1996)

(19) Shertukde, V. V. and Kale, D. D., *J. Polym. Mater.,* **16,** 55, (1999).

(20) Chang, F. C. and Chiang, C. R., *Polymer,* **38,** 19, 4807, (1997).

(21) Kozlowski, M and Bucknall, C. B., *J. Pure. and Appl. Chem.,* **73(6),** 913, (2001).